

AN ABSTRACT OF THE THESIS OF

Shyuer-Ming Shih for the degree of Master of Science in Oceanography

presented on July 19, 1989.

Title: Hydraulic Control of Grain Size Distributions and Differential Transport Rates of Bedload Gravels in Oak Creek, Oregon

Redacted for Privacy

Abstract Approved: _____

Grain-size distributions of gravels transported as bedload in Oak Creek, Oregon, show systematic variations with changing flow discharges. At low discharges the gravel distributions are nearly symmetrical and Gaussian. As discharges increase, the distributions become more skewed and follow the ideal Rosin distribution. The patterns of variations are established by goodness-of-fit comparisons between the measured and theoretical distributions, and by Q-mode factor analysis. Two end members are obtained in the factor analysis, respectively having almost perfect Gaussian and Rosin distributions, and the percentages of the two end members within individual samples vary systematically with discharge.

Transformation from the Gaussian to a Rosin distribution with increasing discharge may be explained by processes of selective entrainment of grains from a bed of mixed sizes. Samples of bed material in Oak Creek follow the Rosin distribution. At high discharges, the transported bedload approaches the grain sizes of that bed-material source and mimics its Rosin distribution. Random-selection processes must be more important to grain entrainment at lower discharges, so that the resulting Gaussian distributions of transported bedload reflect similar distributions of bed stresses exerted by the stream flow.

The results from Oak Creek demonstrate that the competence of the flow is reflected in the entire distribution of transported gravel sizes. A sequence of layers of fluvial gravels, modern or ancient, might show systematic variations between coarse Rosin and finer-grained Gaussian distributions, and these could be used to infer frequencies of various discharges and to establish a relationship to the source sediment.

A differential bedload transport function is formulated utilizing the dependence of two parameters in the Rosin distribution on the flow stress. The total transport rate, which is also a function of the flow stress, is apportioned within the Rosin grain-size distribution to yield the fractional transport rates. The derived bedload function has the advantage of yielding smooth, continuous frequency distributions of transport rates for the grain-size fractions, in contrast to the discrete transport functions which predict rates for specified sieve fractions. A group of differential transport frequency curves can be constructed that reflects a particular stream's bedload transport characteristics. Successful reproduction of the measured fractional transport rates and bedload grain-size distributions by this approach demonstrates its potential in flow-competence estimates, evaluations of differential transport rates of size fractions, and in investigations of downstream changes in bed material grain-size distributions.

Hydraulic Control of Grain Size Distributions and
Differential Transport Rates of Bedload Gravels in Oak Creek, Oregon

by

Shyuer-Ming Shih

A THESIS

submitted to

Oregon State University

in partial fulfillment
of the requirements for
the degree of

Master of Science

Completed July 19, 1989
Commencement June, 1990

APPROVED:

Redacted for Privacy

Professor of Oceanography in charge of major

Redacted for Privacy

Dean of College of Oceanography

Redacted for Privacy

Dean of Graduate School

Date thesis is presented _____ 19 July 1989

Typed by _____ Shyuer-Ming Shih

ACKNOWLEDGEMENTS

I wish to express my sincere appreciation and thanks to my major professor, Dr. Paul Komar for his invaluable support and guidance during my graduate study at Oregon State University and the writing of this thesis.

Special thanks to my committee members, Dr. Joan Oltman-Shay and Dr. Gordan Grant for their helpful comments in reviewing the manuscript. My thanks also to Dr. Donald Amort for serving as graduate representative.

I am grateful to Dr. Nick Pias for his advice on the statistical analyses involved in this study. Appreciation is extended to Dr. Rob Holman and Dr. Erwin Suess for their great lectures that helped me learn more about Marine Geology.

I would also like to thank Dr. C. Christensen as well as Dr. R. Schleyer who provided the computer programs for analyses of the grain-size distributions.

Finally, special thanks to my parents and my wife Ming-Hsia for their love and support.

Funding for this study was provided in part by the Planetary Geology and Geophysics Program, Solar System Exploration Division, NASA. Additional funding was provided by Oregon State University Sea Grant Program, supported by NOAA Office of Sea Grant, Department of Commerce.

TABLE OF CONTENTS

	GENERAL INTRODUCTION	1
CHAPTER 1	HYDRAULIC CONTROLS OF GRAIN-SIZE DISTRIBUTIONS OF BEDLOAD GRAVELS IN OAK CREEK, OREGON	4
	ABSTRACT	5
	INTRODUCTION	7
	MEASUREMENTS AT OAK CREEK	9
	GENERAL VARIATIONS IN DISTRIBUTIONS	13
	GAUSSIAN AND ROSIN DISTRIBUTIONS	17
	FACTOR ANALYSIS OF SIZE DISTRIBUTIONS	25
	SUMMARY AND DISCUSSION	30
	ACKNOWLEDGEMENTS	33
CHAPTER 2	DIFFERENTIAL BEDLOAD TRANSPORT RATES IN A GRAVEL-BED STREAM: A GRAIN-SIZE DISTRIBUTION APPROACH	34
	ABSTRACT	35
	INTRODUCTION	36
	THE OAK CREEK DATA	39
	GRAIN-SIZE DISTRIBUTIONS	42
	TOTAL TRANSPORT RATES OF GRAVELS IN OAK CREEK	50
	TRANSPORT RATES OF GRAIN-SIZE FRACTIONS	55
	COMPARISONS WITH PARKER ET AL. (1982) AND DIPLAS (1987)	59
	NORMALIZATION OF THE RESULTS	62
	SUMMARY AND DISCUSSION	64

REFERENCES	66
APPENDICES	
A. GRAIN-SIZE AND HYDRAULIC PARAMETERS	70
B. ROSIN PAPER	73

LIST OF FIGURES

<u>Figure</u>		<u>Page</u>
1 - 1	Grain-size distributions for the armor (pavement) and subarmor (subpavement) in Oak Creek, and their difference obtained by subtraction.	10
1 - 2	Two time series of grain-size distributions of bedload captured in the vortex trap, illustrating how the distributions change with flow discharge.	14
1 - 3	Frequency curves for the theoretical Rosin and Gaussian distributions.	18
1 - 4	A series of cumulative curves of bedload size distributions on Rosin paper, ordered from right to left by increasing discharge. Distributions of the armor and subarmor samples are plotted at the far left. The theoretical Gaussian distribution graphs as a curve on Rosin paper as shown to the right.	20
1 - 5	Goodness-of-fit values respectively for the Rosin and Gaussian distributions versus the flow discharge.	23
1 - 6	Variations with discharge of the k and s parameters in the Rosin distributions for the bedload samples. The analyses were limited to samples obtained at discharges in excess of 1 m ³ /sec.	24
1 - 7	The first two end members obtained from Q-mode factor analysis of the bedload samples, accounting for 94% of the sample variation.	27
1 - 8	Cumulative curves of the two end members derived from factor analysis (Fig. 1-7) plotted on Rosin paper. The smooth curve for end-member 2 is the ideal Gaussian distribution.	28

1 - 9	Variations with discharge of the proportions of the two end members of Fig. 1-7 in each bedload sample obtained in the Q-mode factor analysis.	29
2 - 1	Histograms of pavement and subpavement in the Oak Creek study reach of Milhous (1973), together with best-fit Rosin distributions.	40
2 - 2	A time series of bedload grain-size distributions collected by Milhous (1973) from Oak Creek during the peak (#58) and waning phases of a flood. Discharges are given in parentheses. The measured distributions, determined by sieving, are presented as histograms, while the smooth frequency curves are the best-fit Rosin distributions.	44
2 - 3	The k parameter of the Rosin distributions fitted to the Oak Creek bedload samples collected at discharges greater than 1 m ³ /sec, compared with the mean bed stress τ and discharge per unit channel width q_w .	45
2 - 4	The dimensionless s spreading parameter of the Rosin distributions fitted to the Oak Creek bedload samples collected at discharges greater than 1 m ³ /sec, compared with the mean bed stress and discharge per unit channel width.	47
2 - 5	A series of frequency curves for ideal Rosin distributions for a range of flow stresses, τ , based on the k and s trends of Figures 2-3 and 2-4 so as to depict variations found in Oak Creek.	49
2 - 6	The mass transport rate of gravel per unit channel width in Oak Creek versus the flow stress. The measurements are the 22 subset of winter-1971 data obtained by Milhous (1973), those collected at discharges greater than 1 m ³ /sec when the pavement is progressively breaking up.	51

- 2 - 7 The mass transport rate of gravel per unit channel width in Oak Creek versus the flow stress. The measurements are the complete set of winter-1971 data obtained by Milhous (1973). 52
- 2 - 8 A Schoklitsch-type analysis of the Oak Creek gravel transport for the subset of winter-1971 data collected by Milhous (1973) when discharges exceeded $1 \text{ m}^3/\text{sec}$. 54
- 2 - 9 Frequency distributions of fractional transport rates of gravels in Oak Creek, calculated for a range of flow stresses, τ . The curves are Rosin distributions with the k and s parameters related to τ in Figure 2-4. The total transport rate is represented by the area under the curve, and was calculated from equation (7a). The dashed line follows the distribution peaks, and shows how it shifts to coarser sizes as the flow stress increases. 57
- 2 - 10 Measured transport rates of different sieve-size fractions as determined directly from the data of Milhous (1973) for the subset of winter-1971 data when discharges were greater than $1 \text{ m}^3/\text{sec}$, versus predicted rates calculated from the Rosin distributions of fractional transport rates analyzed in this study. 58

HYDRAULIC CONTROL OF GRAIN SIZE DISTRIBUTIONS AND DIFFERENTIAL TRANSPORT RATES OF BEDLOAD GRAVELS IN OAK CREEK, OREGON

GENERAL INTRODUCTION

The grain-size distributions of fluvial sediments are primarily determined by the nature of the source materials and the transporting processes. Intuition tells us that if the size distribution of the source materials is known, the size distribution of the bedload must somewhat reflect how the source materials are modified by the transporting processes and, therefore, the character and strength of the transporting medium. This impression has induced numerous studies to relate grain-size distributions to flow hydraulics. One aspect of this is the concept of flow competence, the current's sediment moving ability inferred from the largest particles transported (Baker & Ritter, 1975; Costa, 1983; Komar, 1987). That technique focuses on the maximum sizes entrained and transported, but intuition again tells us that the flow competence should be reflected in the entire size range of transported gravel.

The same concept can be extended to construct predictive models for bedload transport. Most studies have approached this problem by relating the total transport rate to simple hydraulic parameters which determine the stream's sediment-moving capacity. A higher-order consideration involves the development of bedload functions which include predictions of transport rates of the different grain-size fractions represented within the bed material. The movement of grains in a mixture is different from the movement of uniform grains in that small grains can be sheltered by the larger, and the largest particles have greater exposures to the flow. As a result, each size fraction will have its individual transport rate which differs substantially from the total transport of the bed material as a whole. Although it is difficult to study

analytically, the selective transporting effects should be reflected in the changes of grain-size distributions, and can be related empirically to the changes in flow hydraulics.

A problem in grain-size distribution studies of fluvial sediments is that the sediment characteristics are highly variable and difficult to describe analytically. Most researchers have assumed that the bed materials follow a log-normal or Gaussian distribution, and use only one or two grain-size parameters such as the median or some coarse percentile to characterize the sediment as a whole. However, in many fluvial systems the bed material is not log-normally distributed, but instead is bimodal or highly skewed. Any inference of flow hydraulics or formulation of bedload equations based on a single sediment parameter will be inadequate in such streams, and will give inconsistent results from one stream to another, streams which may have the same median grain size, but differ in their overall distributions of bed-material sizes. Bedload transport would be easier to study if the bed materials approach an ideal grain-size distribution and, therefore, can be described by a mathematical function such as Rosin (Rosin and Rammler, 1933) and log-hyperbolic (Bagnold, 1937) distributions. The flow hydraulics can then be related to the size parameters that govern the whole distribution to facilitate the assessment of flow competence or formulation of a bedload transport function.

The objective of this thesis is to examine the grain-size distributions of gravels transported in a stream in order to determine how they relate to hydraulics, and to investigate whether the system variations can serve as the basis for calculations of transport rates of different size fractions. The data employed in these analyses were collected in Oak Creek, Oregon as part of the thesis research of Milhous (1973). Those measurements include grain-size distributions of gravels captured in a bedload trap together with the stream's hydraulic parameters. The grain-size distributions of the gravels show systematic variations with changing flow conditions, and change from

symmetrical Gaussian to skewed Rosin distributions as discharges increase. The re-analysis of those data has an additional interest in that it played the primary role in the gravel-transport examinations of Parker, Klingeman & McLean (1982), which gave rise to the belief that armoring produces a nearly equal mobility of all grain sizes. Therefore, the results of this study will have ramifications to evaluations of bedload transport as well as to interpretations of grain-size distributions.

Chapter 1 establishes the general relationship between grain-size distributions and discharges, and proposes an explanation for the observed transformation in size distributions. The patterns of change are established by goodness-of-fit comparisons with the ideal distributions and by factor analysis. Chapter 2 further quantifies the dependence of the size-parameters on the flow stress, and utilizes the relationship to construct a differential bedload transport function.

CHAPTER 1

Hydraulic Controls of Grain-Size Distributions of Bedload Gravels in Oak Creek, Oregon

ABSTRACT

Grain-size distributions of gravels transported as bedload in Oak Creek, Oregon, show systematic variations with changing flow discharges. At low discharges the gravel distributions are nearly symmetrical and Gaussian. As discharges increase, the distributions become more skewed and follow the ideal Rosin distribution. The patterns of variations are established by goodness-of-fit comparisons between the measured and theoretical distributions, and by Q-mode factor analysis. Two end members are obtained in the factor analysis, respectively having almost perfect Gaussian and Rosin distributions, and the percentages of the two end members within individual samples vary systematically with discharge.

Transformation from the Gaussian to a Rosin distribution with increasing discharge may be explained by processes of selective entrainment of grains from a bed of mixed sizes. Samples of bed material in Oak Creek follow the Rosin distribution. At high discharges, the transported bedload approaches the grain sizes of that bed-material source and mimics its Rosin distribution. Random-selection processes must be more important to grain entrainment at lower discharges, so that the resulting Gaussian distributions of transported bedload reflect similar distributions of bed stresses exerted by the stream flow.

The results from Oak Creek demonstrate that the competence of the flow is reflected in the entire distribution of transported gravel sizes. A sequence of layers of fluvial gravels, modern or ancient, might show systematic variations between coarse Rosin and finer-grained Gaussian distributions, and these could be used to infer frequencies of various discharges and to establish a relationship to the source sediment. With further study, analyses of changing bedload grain-size distributions and their transport rates will lead to a better understanding of downstream variations in grain

sizes of bed sediments and how their distributions reflect the progressive development of textural maturity.

INTRODUCTION

Intuition tells us that size distributions of sediments transported by flowing water must somehow reflect the character and strength of the transporting medium. This impression has induced numerous studies by geologists, first to mathematically describe the grain-size distributions and then attempt to relate them to flow hydraulics. The log-normal or Gaussian distribution is most commonly used, but there also have been proponents for Rosin and hyperbolic distributions. Still other investigators have assumed that complex distributions represent the summation of separate Gaussian distributions.

This basic lack of agreement on how to characterize sediment grain-size distributions has hindered attempts to relate them to flow hydraulics. Best known of such attempts is that introduced by Visher (1969) who focused on "kinks" in the cumulative curves of sand-size distributions. The basic assumption is that these kinks represent transitions between adjacent Gaussian subpopulations, each of which represents a different mechanism of sediment transport. However, other studies suggest that the kinks are not real, that they instead are artificially produced by having plotted the data on log-normal cumulative graph paper rather than on paper representing some other type of distribution (Jackson, 1978; Leroy, 1981; Christiansen, Blaesild & Dalsgaard, 1984). Because of such problems, little agreement exists on hydraulic interpretations of sand-size distributions (Komar, 1986).

The interpretation of distributions of gravels appears more promising. One aspect of this is the concept of flow competence, the measure of a current's sediment moving ability inferred from the largest particles transported (Baker & Ritter, 1975; Costa, 1983; Komar, 1987). That technique focuses on the maximum sizes entrained and transported, but intuition again tells us that the flow's competence should be reflected in the entire size range of transported gravel.

The objective of the present study is to examine the grain-size distributions of gravels transported in a stream in order to determine the basic nature of their distributions and how they change with varying discharge. The data employed in these analyses were collected as part of the thesis research of Milhous (1973). Those measurements include grain-size distributions of gravels captured in a bedload trap together with the stream's hydraulic parameters. The re-analysis of those data has an additional interest in that it played the primary role in the gravel-transport examinations of Parker, Klingeman & McLean (1982), which gave rise to the belief that armoring produces a nearly equal mobility of all grain sizes. Therefore, the results of this study will have ramifications to evaluations of bedload transport as well as to interpretations of grain-size distributions.

MEASUREMENTS AT OAK CREEK

Milhous (1973) obtained measurements of gravel transport in Oak Creek, a small stream in the east central part of the Oregon Coast Range, immediately west of Corvallis. The drainage area above the primary study site is approximately 6.7 km², and the channel length is about 3.5 km. The mean annual discharge is only 0.1 m³/sec, but most of the precipitation occurs during the winter so discharges in that season are generally much greater.

The study of Milhous (1973) involved a relatively straight, 70-m long stretch of stream. Samples of bed material were collected in this reach and sieved to determine the distributions for the armor (pavement) and subarmor (subpavement) given in Figure 1-1. It is seen that an armor layer is well developed in Oak Creek, consisting of a narrow range of coarse clasts, while the subarmor contains a wide range of particle sizes. The contrast is illustrated by the third histogram in Figure 1-1, obtained by subtracting the size distribution of the subarmor from that of the armor. This shows the concentration of particles larger than -5.25ϕ (38 mm) in the armor as opposed to the subarmor; also apparent is the presence of a granule mode in the subarmor centered at about -2.25ϕ (4.8 mm), presumably a matrix fill captured within the pore spaces of the gravel.

A vortex trap was employed to capture the total bedload transported along Oak Creek (Milhous, 1973). This trap consists of a flume with a 30-cm wide opening, placed diagonally across the full stream width. The flume is circular in section so that a vortex is formed which removes the bedload and carries it to a sample box adjacent to the stream. Part of the water discharge is also diverted, and this prevents re-entrainment of the trapped bedload. The use of vortex traps dates back to the 1930s when they were first employed to remove unwanted bedload sediments from irrigation canals. Robinson (1962) summarizes the field and laboratory studies undertaken to improve their design

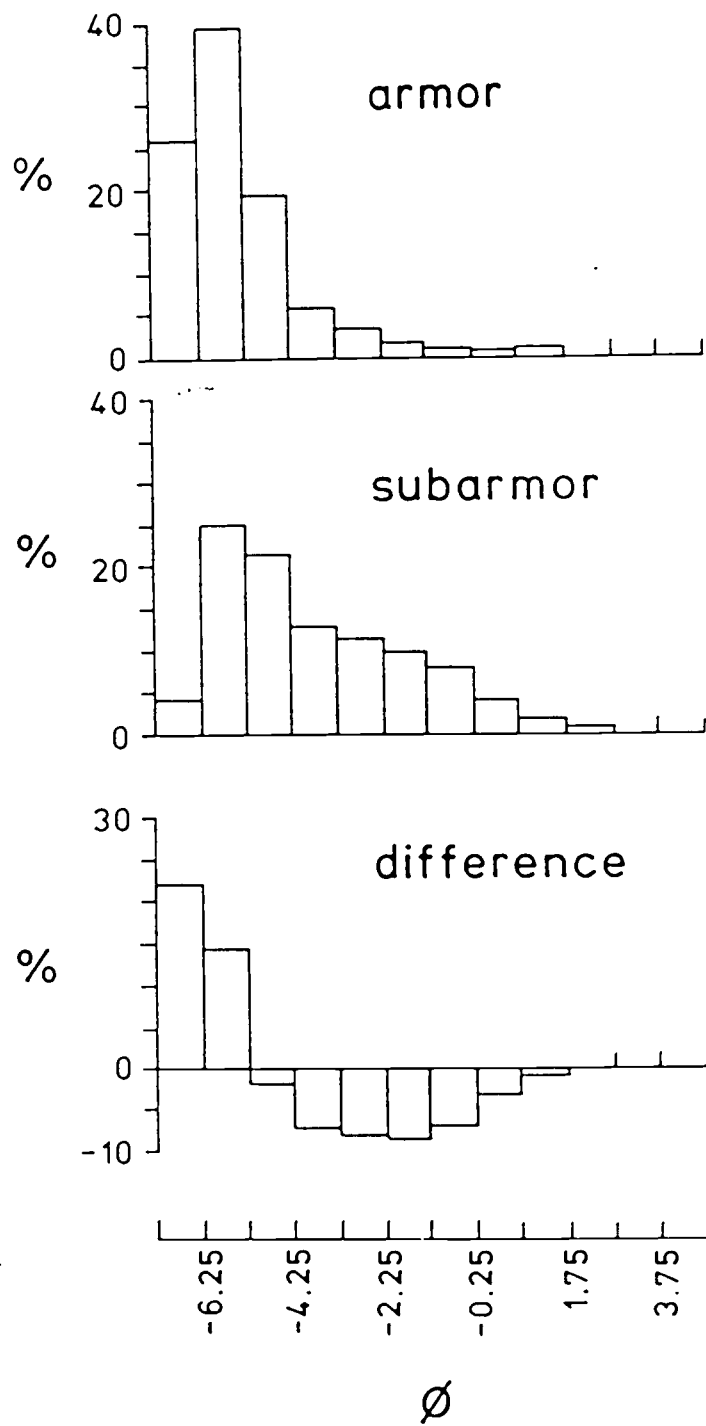


Figure 1-1. Grain-size distributions for the armor (pavement) and subarmor (subpavement) in Oak Creek, and their difference obtained by subtraction.

and effectiveness in capturing bedload. Poreh, Sagiv & Seginer (1970) have systematically studied the sampling efficiency in a series of large-scale flume tests. Detailed analyses were also undertaken by Milhous of the trapping efficiency of the Oak Creek installation, and it was concluded to be at least 95% at typical bedload transport rates. A second trough was placed two feet downstream of the vortex flume in order to act as a backup trough; it captured almost no additional sediment, providing further evidence for the efficiency of the vortex system.

The higher the discharge and hence gravel transport, the shorter the time intervals over which the bedload samples were collected. At the highest transport rates, sampling involved less than 30 minutes, whereas the average sampling interval was about 3 hours. At the very lowest discharges, sampling continued for up to 90 hours. We include all of the measurements in our analyses, but more consideration is given to samples collected at discharges greater than $1 \text{ m}^3/\text{sec}$. Collection of those samples involved less than 3 hours, and therefore are not likely to have been affected by changes in flow hydraulics. In addition, the $1 \text{ m}^3/\text{sec}$ discharge is approximately the flow stage at which the armor pavement begins to break up, while above $2 \text{ m}^3/\text{sec}$ "the whole bed seemed to be in motion" according to the observations of Milhous (1973).

Many of the bedload samples collected in the vortex trap, especially those obtained at higher discharges, weighed over 100 kg. These were processed by first passing them through a 9.5 mm (3/8 inch) sieve. The coarser fraction was then sieved in the field, while a split of the finer material was taken to the laboratory for separate sieving. As tabulated by Milhous (1973), these two divisions are recombined into a single overall size distribution. The ranges of sizes of the bedload gravels are extreme, so that sieving yields 10 to 12 size fractions and therefore reasonably well-defined distributions. This was already seen in Figure 1-1 for the distributions of the bed material.

Milhous (1973) also obtained measurements of the channel geometry and flow hydraulics. The overall channel slope in the study reach is 0.014, and the bottom width averages 3.65 m. The vortex trap is incorporated into a broad-crested weir, which acts as a control for water level at a nearby stilling well to provide a stable stage versus discharge relationship.

Milhous (1973) collected data during three time periods spanning three years. The measurements employed here are his data obtained in January through March 1971. Those data are most useful in the present analysis because of the large range of discharges produced by three floods, yielding significant variations in the quantities and grain sizes of bedload.

GENERAL VARIATIONS IN DISTRIBUTIONS

Two time sequences of size distributions of gravels caught in the vortex trap are given in Figure 1-2. Adjacent to each histogram is the flow discharge measured at the time of sample collection. Series A includes bedload sample #14, obtained when the discharge was $3.4 \text{ m}^3/\text{sec}$, the highest flow during the winter 1971 when sampling was underway. Sample #13 was also obtained during high-flow conditions, just prior to the flood peak. The rest of series A follows the changing grain-size distributions during the waning stage of the flood. It is seen that there is a considerable variation in the sizes of the transported gravel. There are systematic changes in the relative amounts of the several sieve fractions with discharge, the overall effect being an increase in the grain sizes within the bedload at the higher discharges. The trends of changing sizes are particularly evident at discharges greater than $1 \text{ m}^3/\text{sec}$, the flow stage at which the armor pavement begins to break up. In addition to these shifts in sizes of grains being transported, it is apparent in Figure 1-2 that the overall character of the distribution varies with discharge. At lower discharges, the distributions tend to be relatively symmetrical with a visual conformity to the ideal Gaussian distribution. At higher discharges, the distributions are skewed, and become more like those of the bed material (Fig. 1-1).

Series B in Figure 1-2 re-affirms the patterns seen in series A, at least for samples #58 through #62. These again represent the waning phase of the flood, with the maximum discharge of $2.6 \text{ m}^3/\text{sec}$ having occurred during the collection of sample #58. New here is the presence of bimodality seen in samples #56 and #57. These were obtained at discharges of 1.8 and $2.0 \text{ m}^3/\text{sec}$, that is near completion of the break up of the armor pavement and its full mobilization. This suggests that the finer mode might represent part of the matrix fill from within the subarmor. This mode is centered at about 0ϕ (1 mm) (Fig. 1-2), which is somewhat finer than the granule

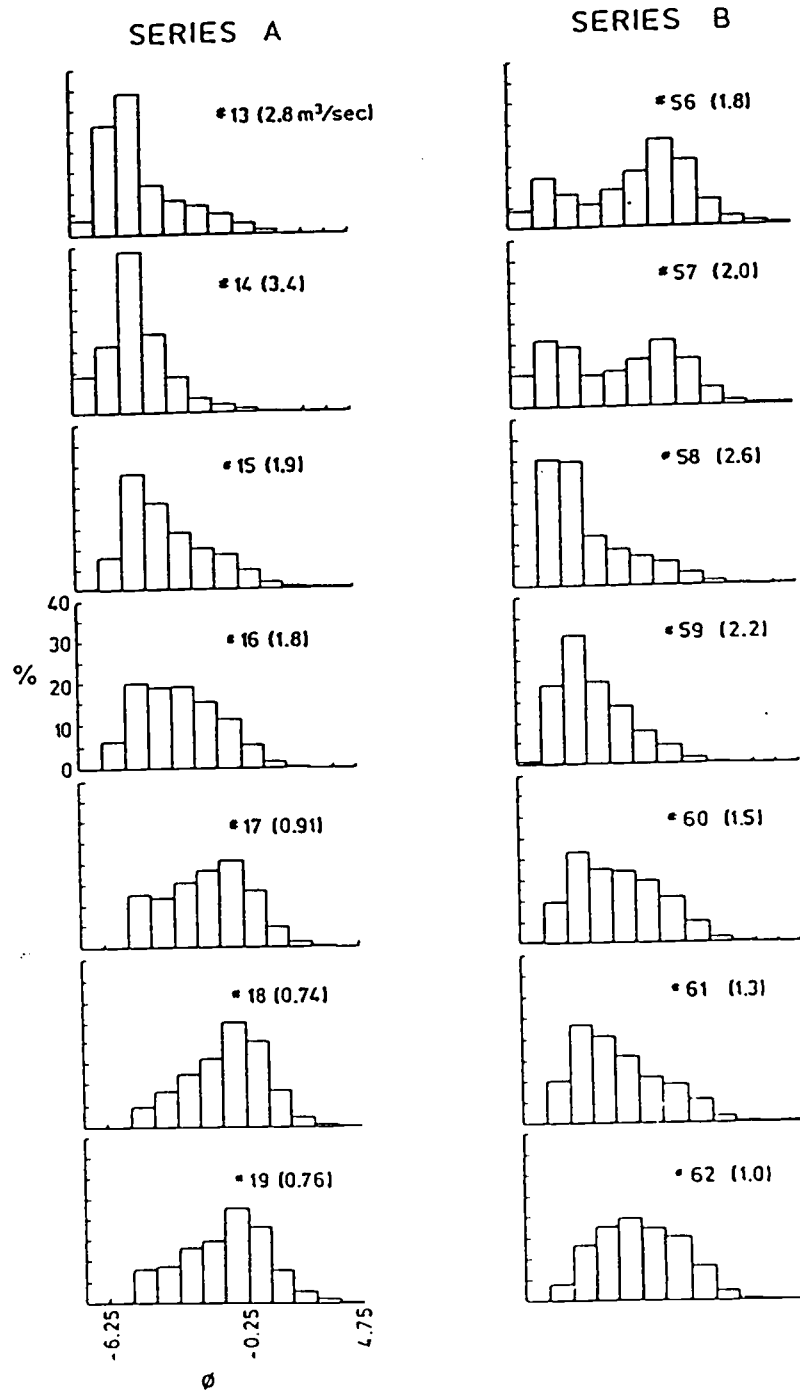


Figure 1-2. Two time series of grain-size distributions of bedload captured in the vortex trap, illustrating how the distributions change with flow discharge.

mode seen in the difference between the armor and subarmor histograms (Fig. 1-1). It is possible that the finer-grained modes of the bimodal distributions are the coarser portions of a suspended load that were captured in the vortex trap since Milhous (1973) found a similar maximum in suspended-load concentrations during stages of increasing flow. However, his recollection is that his samples of suspended sediments were finer grained than the 1 mm mode found in the vortex samples (Milhous, pers. com.). It is possible that the second mode represents a release of finer-grained bedload sizes from the bed-material matrix. The origin of this second mode in the size distributions of the trap samples cannot be resolved at present.

It is necessary to examine whether sampling efficiencies of the vortex trap could have affected the grain-size distributions of the samples to the extent of having produced the increasing skewness at higher discharges. Important is the division between the grain sizes of the bedload versus suspension transport, since the vortex system is designed to trap bedload and almost totally excludes the suspension transport (Poreh et al., 1970). As noted above, Milhous also collected samples of suspended materials at times when the vortex bedload sampler was in operation, and his recollection is that they were finer grained than 1 mm. This recollection is supported by the later measurements of Beschta (1983) in Oak Creek, utilizing a Helley-Smith bedload sampler and a pumping system for the suspended load. Based on numerous samples, Beschta placed the bedload versus suspension grain-size division at about 0.2 mm. The evaluations by Parker et al. (1982) and Diplas (1987) of transport rates of bedload size fractions are consistent down to at least a 0.5 mm grain size, providing indirect evidence that the transition to suspension transport must occur at still finer grain sizes. According to these separate lines of evidence, suspension transport should have affected no more than one or two of the finest fractions of the histograms of Figure 1-2. Of importance in this respect is that for samples such as #13 and #14 collected at high discharges, the decreasing portions of the finer half of the distributions reflect actual

bedload grain sizes rather than decreasing sampling efficiencies due to grain suspension. The detailed study by Poreh et al. (1970) showed that within the range of bedload grain sizes, the sampling efficiency of the vortex trap has almost no dependence on grain size; what little dependence exists, actually favors capture of the smaller sizes over the larger. A final line of evidence is that with increasing discharge, the bedload samples mimic the distribution of the bed material, including the high degree of skewness and progressive fall off of frequencies of the smaller size fractions. Sampling inefficiencies of the vortex trap could not account for such a convergence of bedload and bed material grain-size distributions.

It should be recognized that the changing grain-size distributions seen in Figure 1-2 reflect the relative transport rates of the different size fractions, not their absolute transport rates. Accordingly, as the discharge increases, all sizes that can be moved by the flow are transported at progressively higher rates as shown by the analyses of Parker et al. (1982) and Diplas (1987). This is also true of the finer size fractions, even though their frequencies in the grain-size distributions of the bedload samples decrease with increasing discharge (Fig. 1-2). The observed transformations in grain-size distributions reflect the processes of selective entrainment of grains from a bed of mixed sizes, and ultimately their relative transport rates.

GAUSSIAN AND ROSIN DISTRIBUTIONS

The unimodal distributions of Oak Creek gravels have the appearance of either the symmetrical Gaussian distribution or the skewed Rosin distribution, depending on the flow discharge. In this section we explore in detail the agreement between the measured distributions and these two ideal representations.

Examples of ideal Rosin and Gaussian distributions are shown in Figure 1-3. The cumulative form of Rosin distribution is expressed as

$$R(x) = 100 \exp[-(x/k)^s] \quad (1)$$

where $R(x)$ is the cumulative frequency, that is, the percent which is coarser than x , and k is the mode of the distribution which is positioned at the 36.8 cumulative percent. The dimensionless parameter s governs the spread of the distribution, with the spread decreasing as s increases (s is comparable to the inverse of the standard deviation of the Gaussian distribution).

The Rosin distribution was originally defined by Rosin & Rammler (1933) in a study of crushed powered coal. It subsequently has been shown to describe size distributions of a variety of artificially crushed materials as well as natural products such as jointed bed rock (Kittleman, 1964; Dapples, 1975). Of particular interest here is the application of the Rosin distribution to stream gravels by Ibbeken (1983). Grain-size analyses of gravels from 19 rivers in Calabria, southern Italy, nearly all yielded Rosin distributions. This was interpreted as the distributions reflecting the fractured nature of the source rocks. The samples analyzed by Ibbeken were of stream-bed materials, whereas the Oak Creek data represent bedload captured while in transport.

A special graph paper, similar to log-normal probability paper, has been constructed for the Rosin distribution where grain-size distributions following the

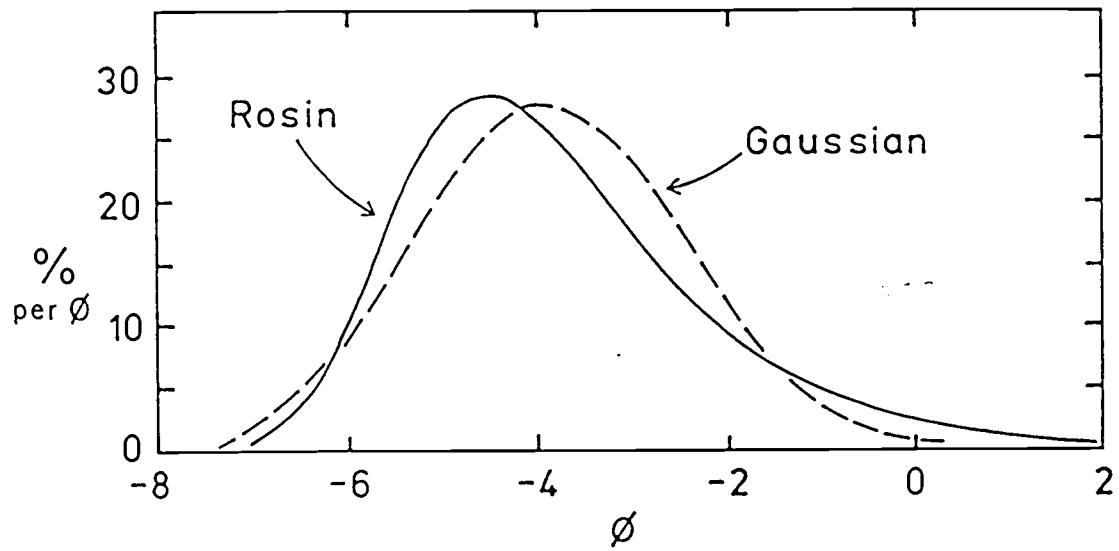


Figure 1-3. Frequency curves for the theoretical Rosin and Gaussian distributions.

Rosin equation (1) plot as straight lines (Geer & Yancy, 1938; Kittleman, 1964). Representative size distributions from Oak Creek are graphed on Rosin paper in Figure 1-4. The bedload samples are arranged from left to right in order of decreasing discharge, but are shifted horizontally so as to avoid superposition. Bimodal distributions are not included in this series. It can be seen that within the bedload samples the distributions become straighter toward the left, that is at higher discharges, confirming that they are approximately of Rosin type. Toward the right and lower discharges, the distributions become concave up. An ideal Gaussian distribution is shown on the far right, and it is seen to have a concave-up curvature when plotted on Rosin paper. The close similarity with the measured distributions at low discharges implies that these bedload samples are approximately Gaussian. The distributions from Figure 1-1 of the armor and subarmor are also plotted in Figure 1-4 as cumulative curves. The subarmor distribution is reasonably straight, indicating some conformity with the Rosin distribution, although there appears to be an excess of coarser fractions. This tendency is even stronger in the armor pavement due to the concentration of large clasts at the surface of the bed in Oak Creek.

The visual impressions gained from Figure 1-4 can be quantitatively assessed by goodness-of-fit determinations. In such analyses, Kittleman (1964) employed an F-test of the linear trend of the cumulative curve on Rosin paper. Ibbeken (1983) took a similar approach with his Calabria data, but discarded some of the size fractions of the coarsest and finest ends because of bimodality and data truncation. A more complex goodness-of-fit measure has been proposed by Schleyer (1987), one which successfully solves the problem of data truncation. However, Schleyer's approach is not easily applied to the Oak Creek distributions, so we have returned to a simpler method which is modified slightly from one used by Rosin & Rammler (1933). The Rosin distribution function is treated as a linear equation after algebraic conversion, and this is compared with the measured cumulative curve to determine the goodness-of-fit parameter:

Figure 1-4. A series of cumulative curves of bedload size distributions on Rosin paper, ordered from right to left by increasing discharge. Distributions of the armor and subarmor samples are plotted at the far left. The theoretical Gaussian distribution graphs as a curve on Rosin paper as shown to the right.

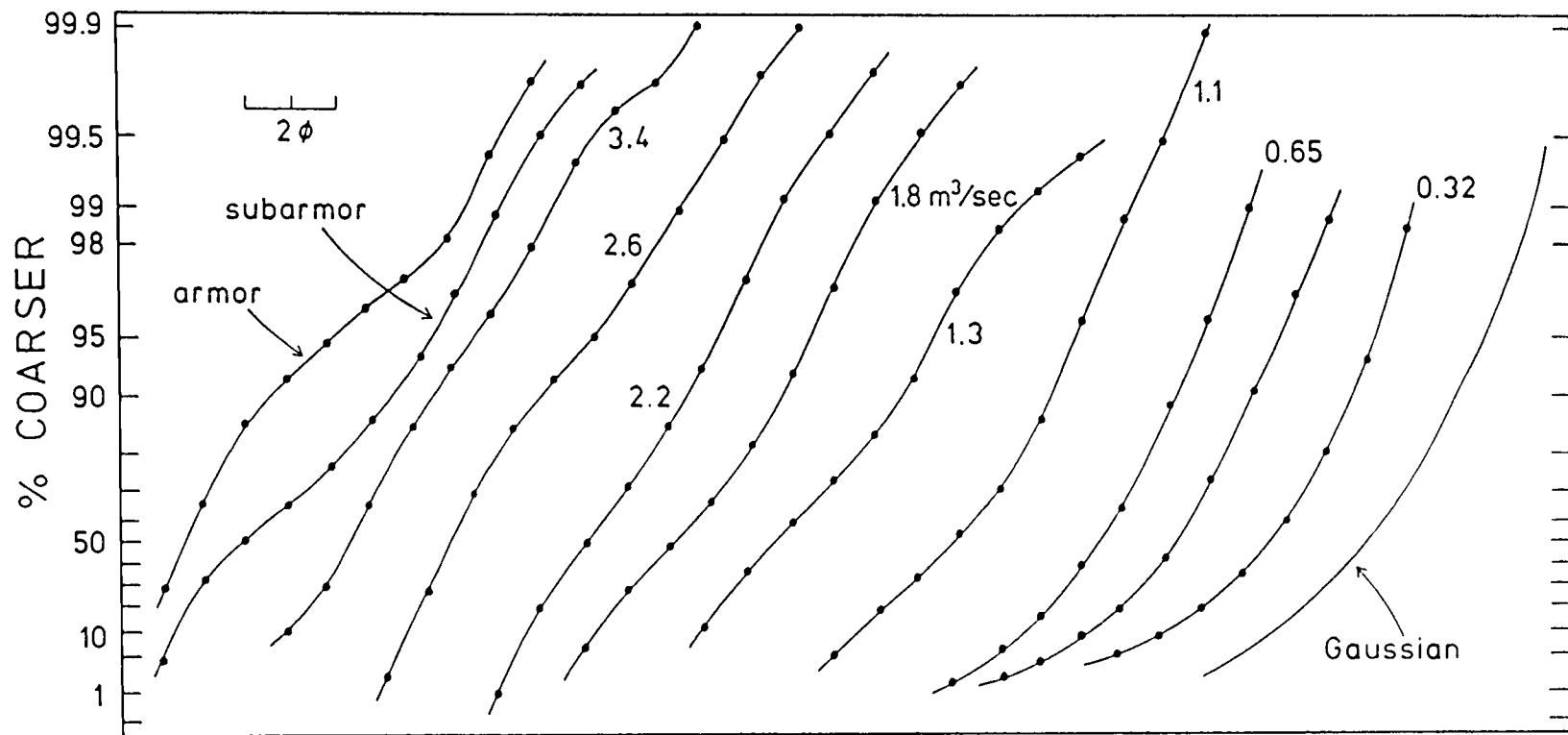


Figure 1-4

$$\text{GOF} = 100 - \frac{\sum |\text{calculated value} - \text{measured value}|}{\text{number of data points} - 1} \quad (2)$$

The GOF values obtained in this way are shown in Figure 1-5 as functions of the flow discharge. The upper diagram is the comparison with the Rosin distribution, and it is seen that agreement increases with increasing discharge. The second diagram, the comparison with the Gaussian distribution, shows just the opposite trend with GOF decreasing at higher discharges. The trends are stronger at discharges greater than 1 m³/sec, that is when the armor layer in the bed material is progressively breaking apart. Bimodal distributions again have been left out of this analysis. The two outliers in the Rosin comparison, marked as X's, are samples 25 and 26 – although not strictly bimodal, they were collected during a transition period immediately following other samples that were bimodal, and this may explain their departure from the trend.

Figure 1-6 shows the variations with discharge of the k and s parameters of the Rosin distribution, equation (1), as fitted to the measured distributions. Only the distributions collected at discharges greater than 1 m³/sec are included, this in effect limiting the data set to distributions which are of Rosin type. The values of k systematically increase with increasing discharge, reflecting the shift in the modes of the distributions toward coarser sizes. The results for s are more scattered, but clearly tend to increase with discharge. Therefore, as the flow strength increases, the mode progressively shifts to coarser sizes and the spread of the distribution narrows. These trends are apparent in the histograms of Figure 1-2.

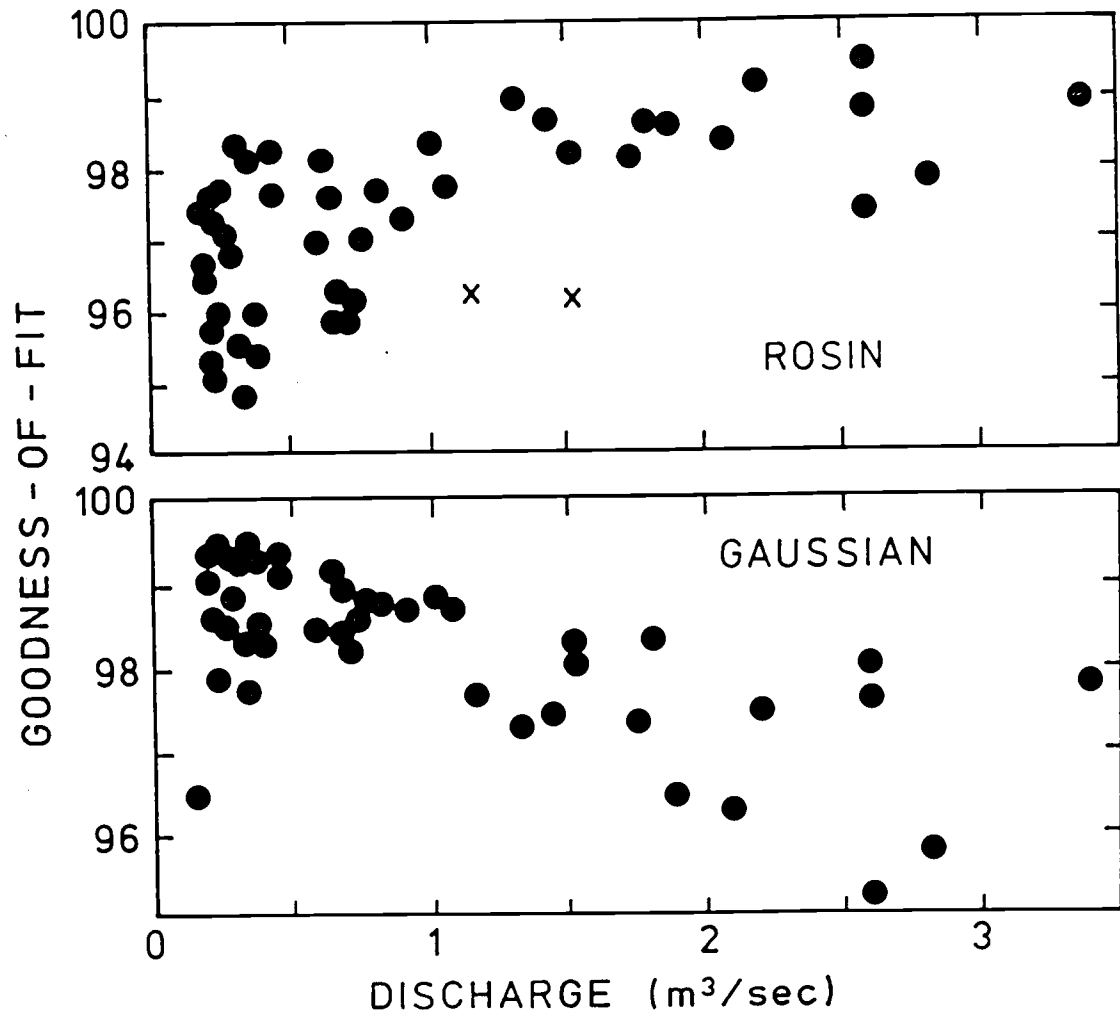


Figure 1-5. Goodness-of-fit values respectively for the Rosin and Gaussian distributions versus the flow discharge.

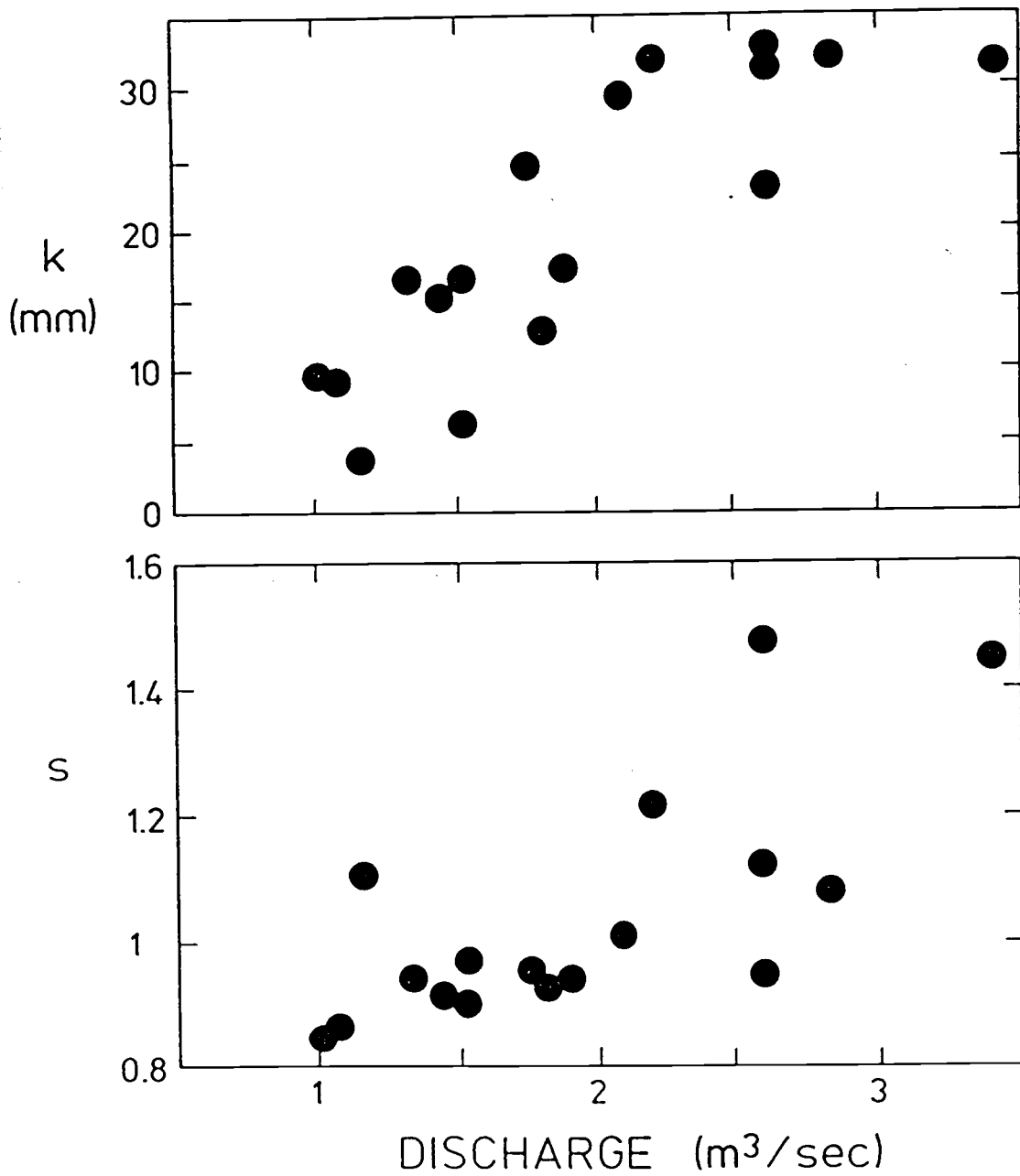


Figure 1-6. Variations with discharge of the k and s parameters in the Rosin distributions for the bedload samples. The analyses were limited to samples obtained at discharges in excess of 1 m³/sec.

FACTOR ANALYSIS OF SIZE DISTRIBUTIONS

Factor analysis provides a still-more objective technique for examining variations in a series of grain-size distributions such as that available from Oak Creek. By treating the various size fractions as different variables, Q-mode factor analysis will determine whether the sample series can be treated as mixtures of end members (Klovan, 1966; Davis, 1986). In our analysis, a modified Q-mode computer program (QROTATE) was employed based on techniques developed by Leinen and Piasias (1984). That program determines the number of important end members, the compositions of the end members, and their abundances within each sample. The QROTATE program is particularly applicable to analyses of grain-size distributions since it yields only positive contributions to samples, obtained by rotating the factor vectors out of negative positions.

The Q-mode factor analysis of the Oak Creek bedload distributions yields two end members, Figure 1-7, which combine to account for 94% of the sample variations. The first end member has the appearance of the Rosin distribution, while the second is similar to a symmetrical Gaussian distribution. The actual comparisons with the theoretical distributions are shown in Figure 1-8 where the end-member distributions are plotted on Rosin cumulative paper. It is seen that the two end members almost precisely follow the theoretical distributions (in each case the goodness-of-fit value exceeds 99%). The proportions of the two end-member factors in each bedload sample are given in Figure 1-9, plotted as functions of the flow discharge. The trends are clear, with the Rosin end member 1 increasing with increasing discharge, reaching 100% Rosin character at the highest discharges, while the Gaussian end member 2 decreases with rising discharge.

The results of factor analysis reaffirm those obtained earlier on the basis of goodness-of-fit evaluations in comparisons with the theoretical distributions. The

division is clearer in the factor analysis since it has the effect of removing random errors by attributing them to factors of lesser importance.

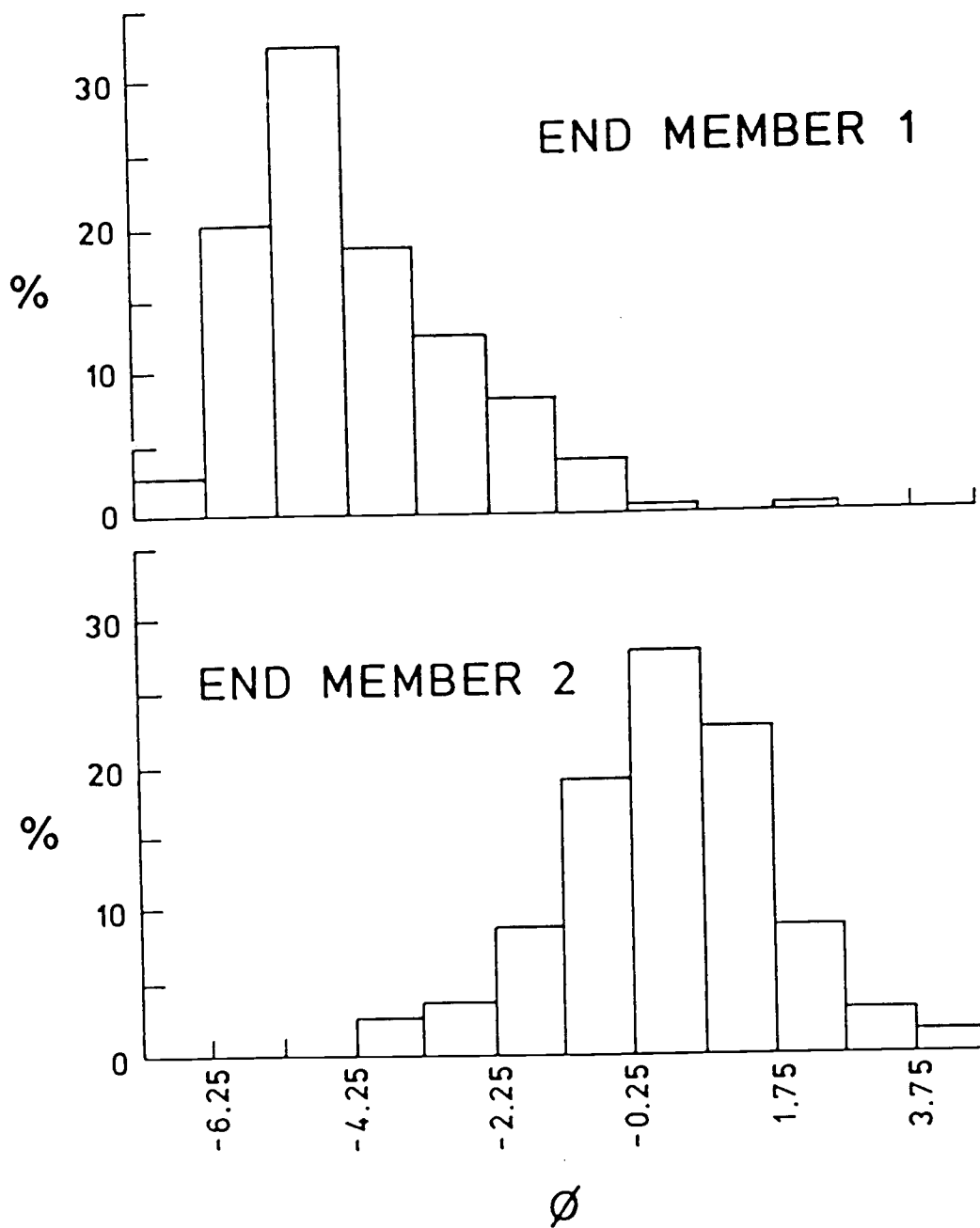


Figure. 1-7. The first two end members obtained from Q-mode factor analysis of the bedload samples, accounting for 94% of the sample variation.

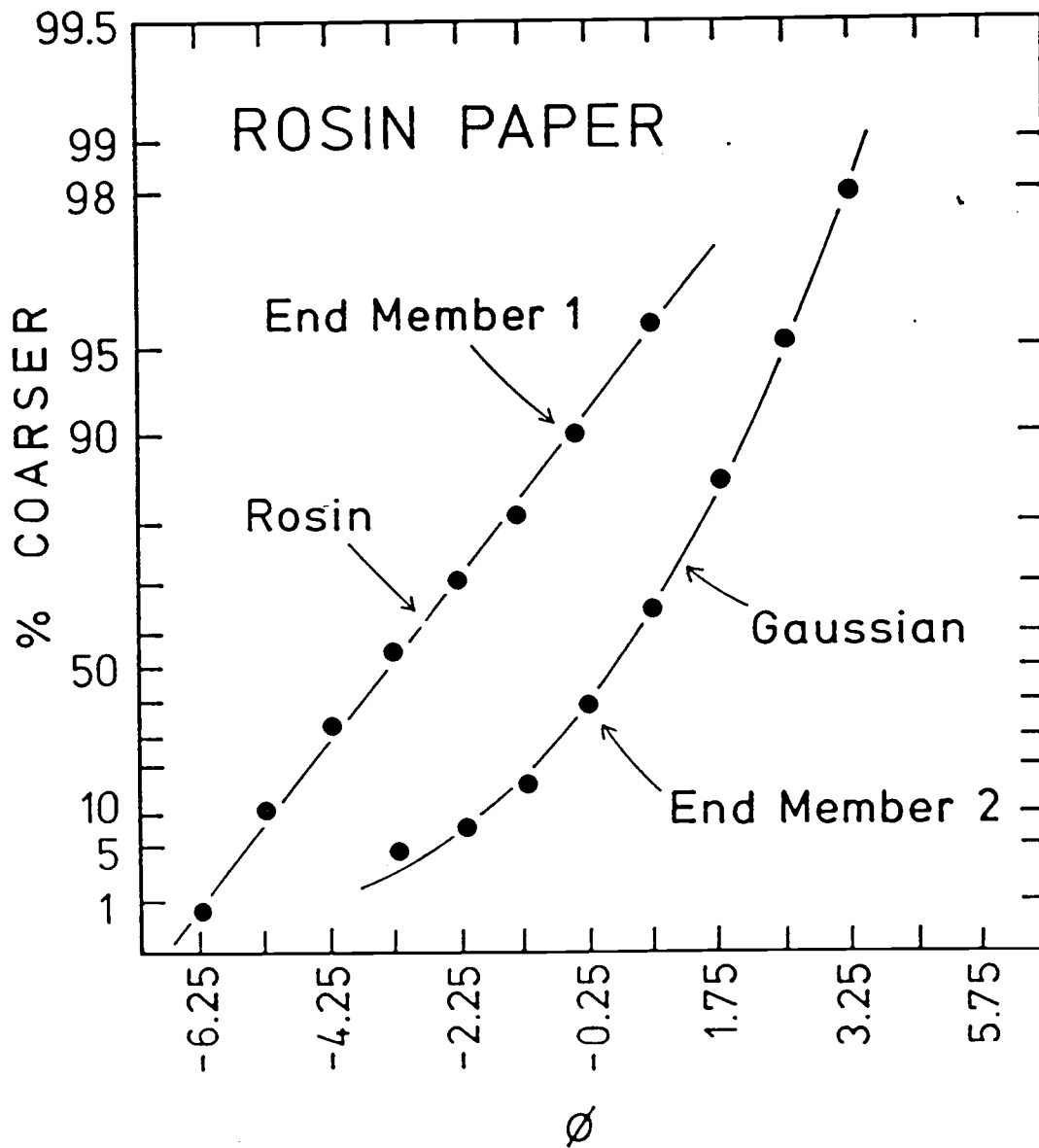


Figure 1-8. Cumulative curves of the two end members derived from factor analysis (Fig. 1-7) plotted on Rosin paper. The smooth curve for end-member 2 is the ideal Gaussian distribution.

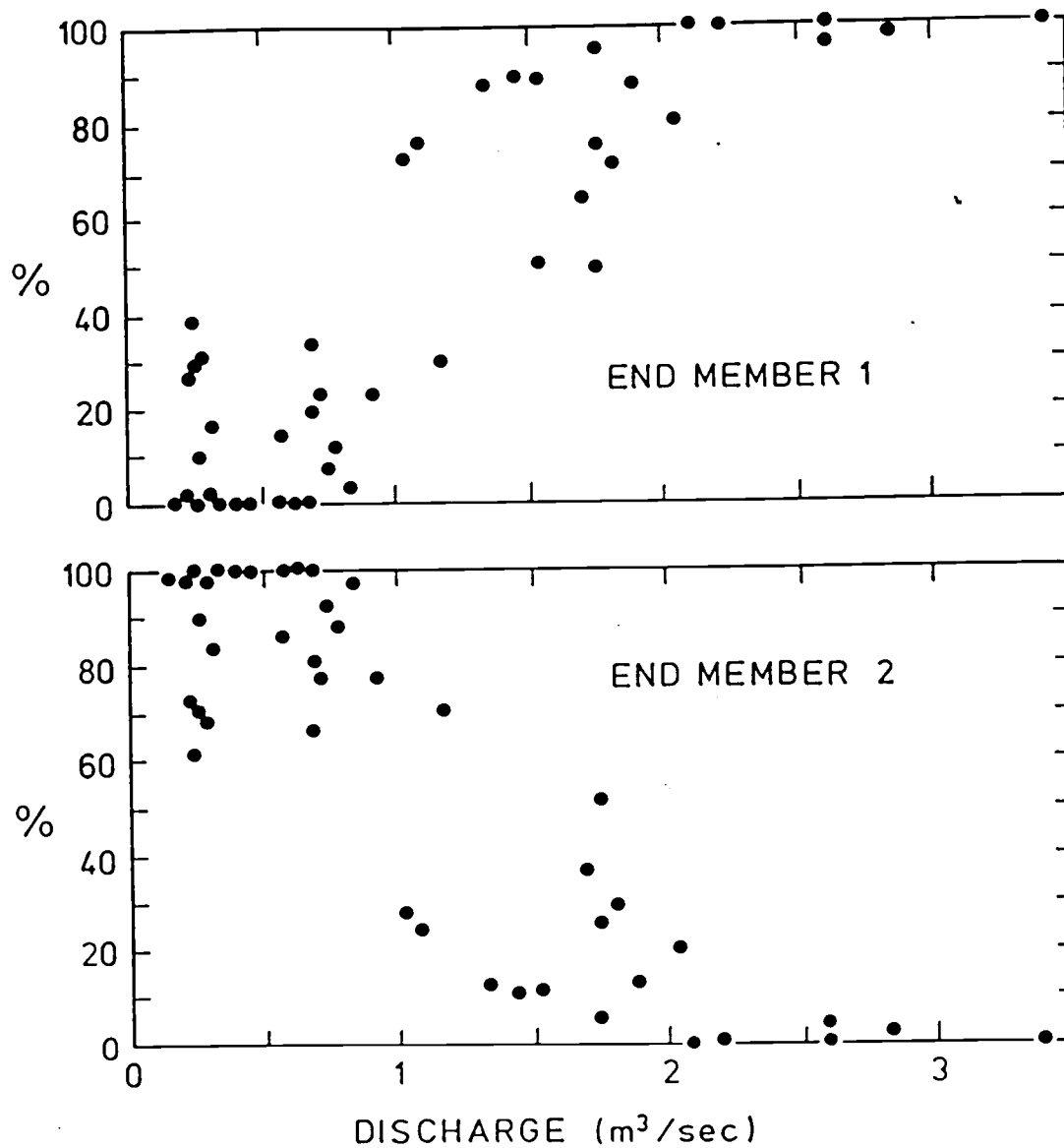


Figure 1-9. Variations with discharge of the proportions of the two end members of Fig. 1-7 in each bedload sample obtained in the Q-mode factor analysis.

SUMMARY AND DISCUSSION

The analyses have revealed significant variations in the grain-size distributions of transported gravels in Oak Creek, changes which correlate with the hydraulics of the flow. Although the trends examined here only involved the flow discharge, alternate choices for evaluating the flow hydraulics could have been the mean shear stress, velocity or flow power. The measured grain-size distributions were limited to comparisons with the ideal log-normal Gaussian and Rosin distributions. Although we have not presented the results, the measured distributions were also compared with the log-hyperbolic distribution developed by Bagnold (1937), Barndorff-Nielsen (1977) and related studies. This analysis demonstrated that as the discharge increases, the mode (v) of the hyperbolic distribution shifts to coarser sizes, and the slope of the finer linear asymptote (ϕ) decreases; it was also apparent that the coarser linear asymptote (γ) systematically increases, but the values are uncertain at high discharges where they are established by only 3 or 4 sieve sizes.

The data of Milhous (1973) have been used in flow-competence considerations, analyses which showed that the sizes of the largest particles transported increase with increasing mean-flow stresses (Komar, 1987). It is now apparent that the entire distribution and range of transported sizes respond to and reflect the competence of the flow, not just the maximum particle sizes. The shift in the mode k of the Rosin distribution with increasing discharge, Figure 1-6, can be viewed as a type of flow-competence correlation. The shift in end members of the factor analysis with discharge, Figure 1-9, is another competence indicator, though one that differs from the traditional approach which involves specific grain-size parameters such as the largest particle transported. This suggests the possibility of using grain-size distributions, as analyzed here, in examinations of flood frequencies recorded in fluvial deposits, modern or ancient. The grain-size distributions from a series of depositional layers might show

systematic variations between coarse Rosin and finer-grained Gaussian distributions, and these could be used to infer the relative frequencies of various discharges responsible for the deposits.

The systematic shifts in the nature of the bedload size distributions in Oak Creek demonstrate that the grain-entrainment processes must be complex and depend on flow stage. At high discharges, nearly all sizes of materials in the bed are mobilized by massive non-selective entrainment, so that the resulting grain-size distribution of bedload reflects the bed-material source. This is apparent in a comparison between Figure 1-1 for the stationary bed material and the distributions in Figure 1-2 for bedload at high discharges. The Rosin shapes are very similar, but it is noteworthy that there is still a shift in ranges of sizes – in all cases the bedload is finer grained than the bed material. At lower discharges, the bedload distributions are Gaussian and no longer mimic the bed-material Rosin distribution. It may be that the distribution of bed shear stresses exerted by the stream flow is now more important in the grain-by-grain entrainment, the bed no longer being fully mobilized. It is known that temporal variations in bed stresses are approximately Gaussian distributed (Grass, 1971), so it is possible that the resulting size distributions of randomly entrained grains similarly end up Gaussian in character.

The analyses of bedload gravels in Oak Creek also have ramifications to downstream changes in bed-material size distributions and to the related concept of a progressive development of textural maturity. This latter concept was introduced by Krumbein and Tisdell (1940), and involves the hypothesis that at an immature stage, the grain-size distribution is represented by Rosin's "crushing law", while the ultimate maturity following transport is a Gaussian distribution. It is apparent from our results, where the character of the bedload size distribution depends on the flow discharge, that the development of textural maturity involves a complexity of processes integrated over a long period of time. In their studies of river gravels in Calabria,

Ibbeken (1983) and Schleyer (1987) demonstrated that the bed gravels usually follow a Rosin distribution while the sand component is Gaussian. The gravel distributions were similar to those of jointed and weathered source rocks, so it was concluded that the river gravels retained a source-specific character while the sand fractions had developed a secondary transport-specific distribution which is Gaussian. This interpretation appears to conform with our observations in Oak Creek. Although size determinations have not been established for the original rock-source materials, the bed gravel in Oak Creek is clearly Rosin in character (Figure 1-1). Wolcott (1988) has analyzed two bed-material samples up to 7.5 km downstream of the vortex trap, and these reveal a decrease in gravel sizes while still retaining a Rosin character (there is no sand mode at that channel distance). Therefore, the transport at higher flow stages of gravels having Rosin distributions apparently yields bed materials further downstream which retain the Rosin form of the original source even though the grain sizes are reduced. In contrast, the selective transport of finer fractions as bedload at lower flow stages occurs in the form of Gaussian grain-size distributions, and this could yield a separate transport-specific Gaussian mode as found by Ibbeken for bed material in the Calabrian streams. In the lower reaches of Oak Creek, the gravel bed material gives way to sand (Wolcott, 1988); although no grain-size analyses have been performed, it is likely that the distribution of that sand is Gaussian.

Additional studies are planned to examine downstream changes of bed-material grain-size distributions in Oak Creek, and to analyze the patterns in terms of gravel-transport rates and grain abrasion. Those investigations should help answer questions concerning the evolution of grain-size distributions with progressive transport, and how those distributions might reflect increasing textural maturity as they evolve from a source-specific to a transport-specific character.

ACKNOWLEDGEMENTS

This work was undertaken with support from the Planetary Geology and Geophysics Program, Solar System Exploration Division, NASA. We would like to acknowledge the assistance of Robert Milhous during our many phone conversations concerning his thesis research in Oak Creek, of R. Schleyer and C. Christiansen who provided computer programs for analyses of the grain-size distributions, and of J. Wolcott who supplied us with his original data on grain-size distributions of bed material in Oak Creek.

CHAPTER 2

Differential Bedload Transport Rates in a Gravel-Bed Stream: A Grain-Size Distribution Approach

ABSTRACT

The grain-size distributions of bedload gravels in Oak Creek, Oregon, follow the ideal Rosin distribution at flow stages which exceed that necessary to initiate breakup of the pavement in the bed material. The distributions systematically change with increasing flow discharges and bed stresses such that the grain sizes increase while the spread of the distribution decreases. A differential bedload transport function is formulated utilizing the dependence of two parameters in the Rosin distribution on the flow stress. The total transport rate, which is also a function of the flow stress, is apportioned within the Rosin grain-size distribution to yield the fractional transport rates. The derived bedload function has the advantage of yielding smooth, continuous frequency distributions of transport rates for the grain-size fractions, in contrast to the discrete transport functions which predict rates for specified sieve fractions. A group of differential transport frequency curves can be constructed that reflects a particular stream's bedload transport characteristics. Successful reproduction of the measured fractional transport rates and bedload grain-size distributions by this approach demonstrates its potential in flow-competence estimates, evaluations of differential transport rates of size fractions, and in investigations of downstream changes in bed material grain-size distributions.

INTRODUCTION

Most studies seeking predictive models for bedload transport in streams have focused on relationships between the total transport rate and simple hydraulic parameters which determine the stream's sediment-moving capacity. A higher-order consideration involves the development of bedload functions which include predictions of transport rates of the different grain-size fractions represented within the bed material. The movement of grains in a mixture is affected by the other particles since small grains can be sheltered by the larger, and the largest particles have greater exposures to the flow. As a result, each size fraction will have its individual transport rate which differs substantially from the total transport of the bed material as a whole.

Einstein (1950) approached this problem by introducing a "hiding factor" determined empirically as a function of the ratio of the grain diameter to a characteristic particle size for the mixture as a whole. Proffitt and Sutherland (1983) have modified two existing bedload formulas and proposed an "exposure correction" for each size fraction to account for deviations from the transport rates calculated by the unmodified bedload transport formulas. Their determination of the "exposure correction" basically follows the same reasoning as Einstein (1950).

A problem in developing bedload-transport relationships for grain-size fractions is that the sediment characteristics are highly variable and difficult to describe analytically. Most researchers have assumed that the bed material follows a log-normal or Gaussian distribution, and use only one or two grain-size parameters such as the median or some coarser percentile to characterize the sediment as a whole. However, in many fluvial systems the bed material is not log-normally distributed, but instead is bimodal or highly skewed. Bedload equations based on a single sediment parameter will be inadequate in such streams, and will give inconsistent results from

one stream to another which may have the same median grain size but differ in their overall distributions of bed-material sizes.

Bedload transport would be easier to study if the bed materials approach an ideal grain-size distribution and, therefore, can be described by a mathematical function. This appears to be the condition in gravel-bed streams where the observed distributions are usually skewed with an extreme departure from log-normality, the distributions instead more closely following the ideal Rosin form (e.g., Ibbeken, 1983). We have analyzed the Oak Creek data collected by Milhous (1973), and found that the bed material follows the Rosin distribution (Chapter 1). We also established that as the flow discharge increases in Oak Creek, the grain-size distributions of the bedload systematically change from log-normal Gaussian to Rosin, while becoming progressively coarser. At the highest discharges, the distributions of the bedload mimic the Rosin distribution of the bed material.

The objective of this paper is to investigate whether the systematic variations of bedload grain-size distributions observed in Oak Creek can serve as the basis for calculations of transport rates of different size fractions. The approach will rely on the Rosin distribution and how its parameters depend on the flow discharge and bed stress. The total transport rate, which is also a function of the discharge or stress, is then apportioned within the distribution of grain sizes of the Rosin distribution to yield frequency curves for the differential transport rates of the spectrum of grain sizes. The Oak Creek data of Milhous (1973) will again be employed in these analyses. Parker et al. (1982) and Diplas (1987) similarly relied on the measurements by Milhous (1973) in their development of empirical approaches for calculations of fractional transport rates of gravels in streams. Our approach differs significantly in methodology from their techniques, and yields complete frequency curves rather than being limited to the specific sieve-size fractions reported by Milhous (1973). We also devote more attention to changing bedload grain-size distributions as well as to transport rates, since

this holds the key to flow-competence evaluations and to studies of downstream fining of bed-material grain sizes.

THE OAK CREEK DATA

Oak Creek is a small gravel-bed stream in the east central part of the Oregon Coast Range, immediately west of Corvallis. The mean annual discharge is only $0.1 \text{ m}^3/\text{sec}$, but most of the precipitation occurs during the winter so discharges of that season are much greater. The bed material is mainly basalt gravel, and decreases in size along the length of the stream (Milhous, 1973; Wolcott, 1988). There is a well-developed pavement and subpavement (Parker et al., 1982), and histograms representative of the study site are shown in Figure 2-1. The median of the pavement is about 60 mm, while the subpavement is 20 mm.

The study of Milhous (1973) involved a relatively straight, 70-m long stretch of stream, which is flume-like in cross section with a 3.6 m uniform width. The overall channel slope in the study reach is 0.014. A vortex trap was employed by Milhous to capture the entire bedload transported along the stream. This trap consists of a flume with a 30-cm wide opening, placed diagonally across the full stream width. Detailed analyses were undertaken by Milhous of the efficiency of this system, and it was concluded to be at least 95% at typical bedload transport rates. At times of highest discharge and gravel transport, sampling involved about 30 minutes, whereas the average sampling interval was about 3 hours. Samples of the bedload typically weighed over 100 kg. These were sieved by Milhous to establish grain-size distributions of the bedload, permitting calculations of fractional transport rates (Parker et al., 1982; Diplas, 1987) and examinations of variations in the grain-size distributions.

Milhous (1973) noted that the bed pavement begins to break up at a discharge of about $1 \text{ m}^3/\text{sec}$, and that above $2 \text{ m}^3/\text{sec}$ "the whole bed seemed to be in motion." The measured bedload transport rates and size distributions are more systematic and less scattered above this $1 \text{ m}^3/\text{sec}$ level than at lower flow stages, so the analyses presented

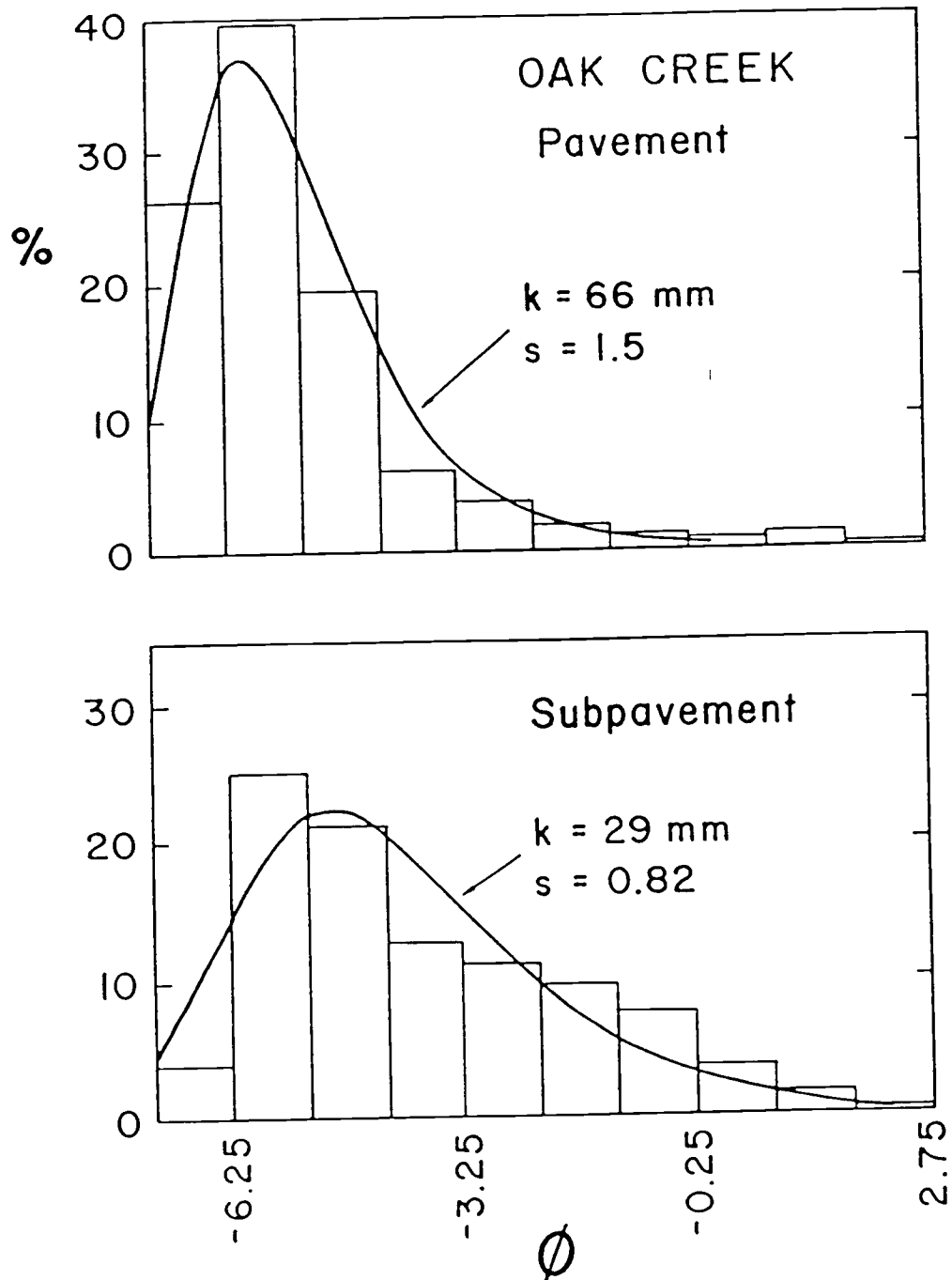


Figure 2-1. Histograms of pavement and subpavement in the Oak Creek study reach of Milhous (1973), together with best-fit Rosin distributions.

here will concentrate primarily on the data gathered during the higher flows. The data used were those collected by Milhous during January through March 1971, his "winter-1971" data. There are 66 samples, with 22 captured at discharges higher than 1 m³/sec. Parker et al. (1982) and Diplas (1987) similarly limited their analyses to these 22 measurement sets.

GRAIN-SIZE DISTRIBUTIONS

The Oak Creek bed-materials and bedload samples collected at discharges greater than 1 m³/sec have been shown to follow the ideal Rosin distribution (Chapter 1). The Rosin distribution was discovered by Rosin and Rammler (1933) in an investigation of crushed coal, and has been supported theoretically by Bennett (1936) on the basis of a model involving random grain fracturing. The distribution is given mathematically as

$$R(x) = 100 \exp[-(x/k)^s] \quad (1)$$

where $R(x)$ is the cumulative percent in weight for materials coarser than size x . The parameter k is the mode of the distribution, and is positioned at $R(k) = 36.8$ cumulative percent. It determines the overall coarseness of the sediment. Note that x and k must have the same units, and it is necessary that in computations they be the original linear units (millimeters, etc.) rather than derivative units (such as the phi scale used by geologists). The second parameter s is a dimensionless factor that controls the overall spread of the distribution. The greater the value of s , the narrower the spread, so it acts much like the inverse of the standard deviation in the Gaussian distribution.

The frequency curve for the Rosin distribution is derived by differentiating $100 - R(x)$, the percent finer than x , to obtain

$$f(x) = 100 (s/k)(x/k)^{s-1} \exp[-(x/k)^s] \quad (2a)$$

On the logarithmic ϕ scale, the frequency curve becomes,

$$f(\phi) = 100 (\log_e 2) s (2^{-\phi}/k)^s \exp[-(2^{-\phi}/k)^s] \quad (2b)$$

Frequency curves are shown in Figure 2-1 compared with the histograms of the pavement and subpavement bed materials in Oak Creek. It is seen that the ideal Rosin distributions have the same pronounced skewness as the bed materials, and clearly would depart significantly from a log-normal Gaussian distribution which must be symmetrical. The fitting of the ideal Rosin distribution to a measured distribution can be done numerically by calculating best-fit k and s parameters (Kittleman, 1964;

Schleyer, 1985). There is also a special graph paper, similar to log-probability paper, wherein the Rosin distribution plots as a straight line (Geer and Yancy, 1938; Kittleman, 1964).

Figure 2-2 shows a series of histograms and best-fit Rosin distributions for bedload samples collected during the falling stage of a flood. Sample #58 was obtained at the peak of stream flow when the discharge was 2.6 m³/sec. This series illustrates how the range of grain sizes and distribution form of the bedload samples vary with discharge. It is apparent that the peaks of the distributions shift towards coarser sizes as the discharge increases, and that the distributions progressively develop a skewed form. The distribution of sample #58 is close to the distributions of the bed materials, Figure 2-1, both in form and grain-size range. As the discharge decreases to 1 m³/sec, the distributions become more symmetrical, and begin to take on the form of the log-normal Gaussian distribution. This trend of increasing conformity with the Gaussian distribution continues for samples collected at discharges below 1 m³/sec (Chapter 1).

The k and s parameters of the Rosin distributions have been determined for 17 of the 22 bedload samples collected at discharges in excess of the 1 m³/sec level required for breakup of the bed pavement, and are plotted in Figure 2-3 as a function of the flow stress. The remaining 5 samples are distinctly bimodal, and therefore have not been included. These bimodal samples occurred during the increasing stages of floods, and appear to be due to the release of a finer-grained second mode from the matrix fill of the subpavement as the pavement is entrained (Chapter 1).

The primary correlation of k in Figure 2-3 is with the mean bed stress calculated with the Duboys equation from the flow depth and water-slope measurements tabulated by Milhous (1973). A scale for the discharge per unit width, q_w , is also given, based on the log-log least-squares regression

$$q_w = 2.51 \times 10^{-4} \tau^{2.18} \quad (3)$$

where the units are respectively m³/m·sec and Newtons/m². The trend of k is readily

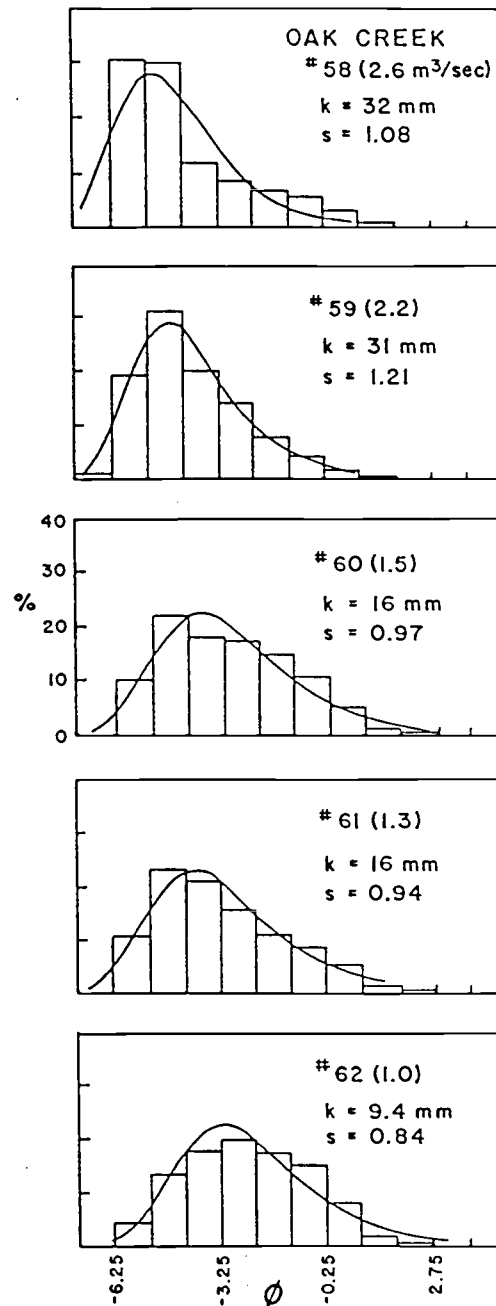


Figure 2-2. A time series of bedload grain-size distributions collected by Milhous (1973) from Oak Creek during the peak (#58) and waning phases of a flood. Discharges are given in parentheses. The measured distributions, determined by sieving, are presented as histograms, while the smooth frequency curves are the best-fit Rosin distributions.

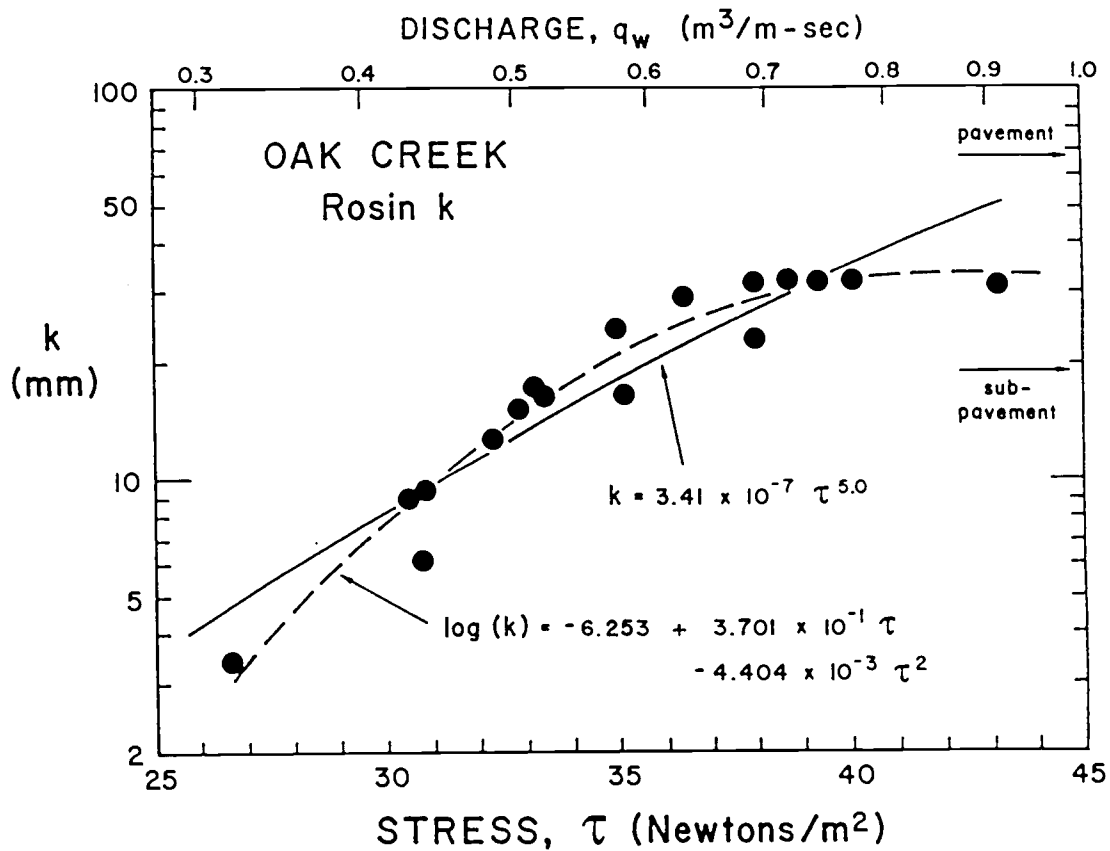


Figure 2-3. The k parameter of the Rosin distributions fitted to the Oak Creek bedload samples collected at discharges greater than $1 m^3/sec$, compared with the mean bed stress τ and discharge per unit channel width q_w .

apparent in Figure 2-3, yielding

$$k = 3.41 \times 10^{-7} \tau^{5.00} \quad [R^2 = 0.876] \quad (4a)$$

The correlation with the discharge is

$$k = 62.7 q_w^{2.30} \quad (4b)$$

These relationships specify the shift in the peaks of the Rosin distributions of the bedload samples to coarser sizes as the flow stress and discharge increase. Although the fit of these relationships is statistically very good, as plotted in Figure 2-3 the k trend appears to have more curvature. This is brought out in that, for convenience, we have plotted the measurements as $\log(k)$ versus linear τ , while the above regressions are based on a log-log best fit. However, one would expect k to level off as the flow increases since ultimately it is unlikely to exceed the k values of the bed material (combined pavement and subpavement); the k values for the pavement ($k = 65$ mm) and subpavement ($k = 30$ mm) are shown as arrows on the right side of the diagram. The dashed curve in Figure 2-3 is for the regression relationship

$$\log_{10}(k) = -6.253 + 3.701 \times 10^{-1} \tau - 4.404 \times 10^{-3} \tau^2 \quad [R^2 = 0.94] \quad (5)$$

which levels off at $k \approx 30$ to 40 mm and follows the curvature of the data better than equation (4a).

The trend of the distribution factor s is more scattered than k (Fig. 2-4), and there are three distinct outliers. The general increase in scatter is due to the fitting of the ideal Rosin distribution to the measured data being relatively insensitive to this parameter. One of the outlier samples was collected immediately after other bedload samples were bimodal, and its distribution may have been affected by the addition of fines even though it did not have a distinct second mode. The other two outliers are for samples collected at high discharges which produced markedly skewed and narrow distributions. The curve

$$s = 0.038 \tau^{0.91} \quad [R^2 = 0.74] \quad (6a)$$

fitted to the data in Figure 2-4 did not include these three outliers. The relationship to

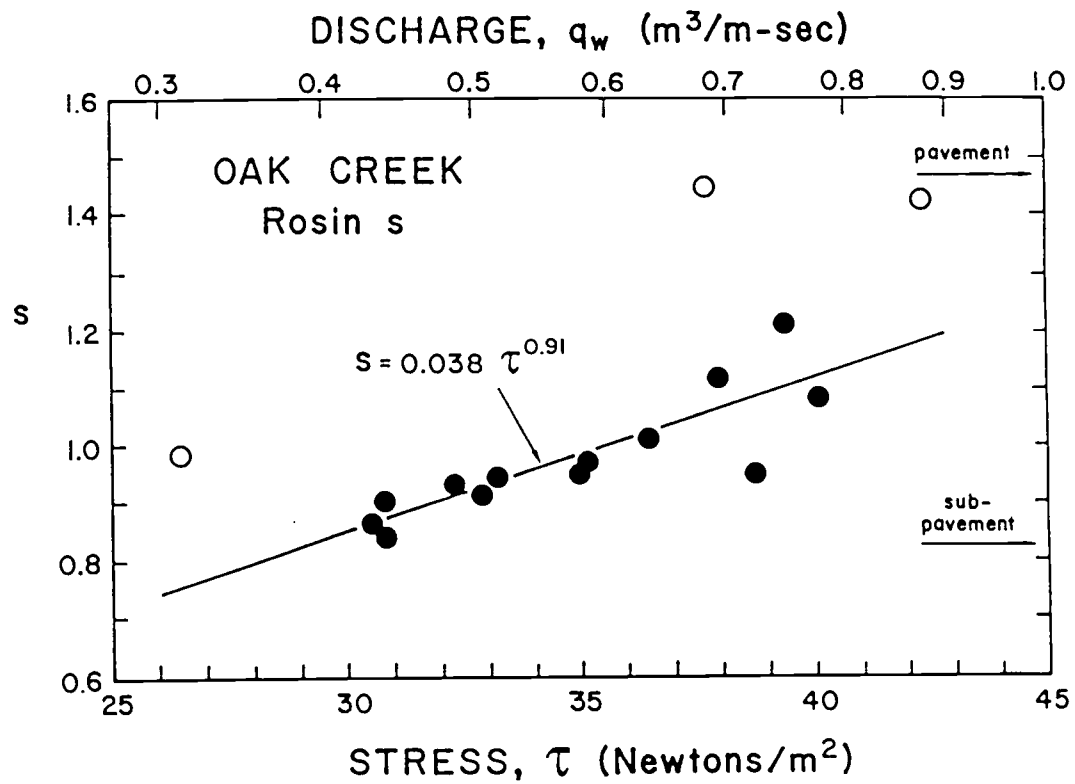


Figure 2-4. The dimensionless s spreading parameter of the Rosin distributions fitted to the Oak Creek bedload samples collected at discharges greater than $1 m^3/sec$, compared with the mean bed stress and discharge per unit channel width.

the discharge is

$$s = 10.04 q_w^{0.42} \quad (6b)$$

It would again be expected that s for the bedload samples might level off to some value intermediate between those of the pavement and subpavement. However, the respective values for the pavement ($s = 1.5$) and subpavement ($s = 0.82$) are sufficiently different that it is not possible to establish what this ultimate s value for the bedload might be. Extrapolation of the curve of equation (6a) to high stresses indicates it might be on the order of $s \approx 1.2$ (Figure 2-4).

These dependencies of k and s on τ and q_w can be used to predict grain-size distributions of bedload in Oak Creek. Most important is the change in k , the position of the mode. The form of the distribution is relatively insensitive to s , so its value is less critical in evaluating the changing grain-size distributions. The prediction of size distributions is illustrated in Figure 2-5 for five flow-stress levels ranging from 25 to 45 Newtons/m². As seen in the original bedload histograms of Figure 2-2, the frequency curves of the calculated Rosin distributions rapidly shift to coarser sizes and develop a skewed form as the flow stress increases. The overall increase of k is from 4.65 to 50 mm, more than a factor 10 change, while the increase in the frequency at the mode is only 17 to 32 %/φ. The degrees of spread of the calculated distributions decrease as the flow stress increases due to the progressively larger values of s .

The curves in Figure 2-5 represent continuous distributions which show the relative frequencies of the different sizes, and are an obvious improvement over the histograms which must be limited to the specific series of sieve sizes that happened to be employed in the analyses. Furthermore, the distributions can now be described by the mathematical expressions of equations (1) and (2), which depend on only two parameters, k and s . The empirical equations (4) through (7) summarize how those parameters change with varying flow hydraulics. This greatly simplifies analyses of the changing bedload grain-size distributions in Oak Creek.

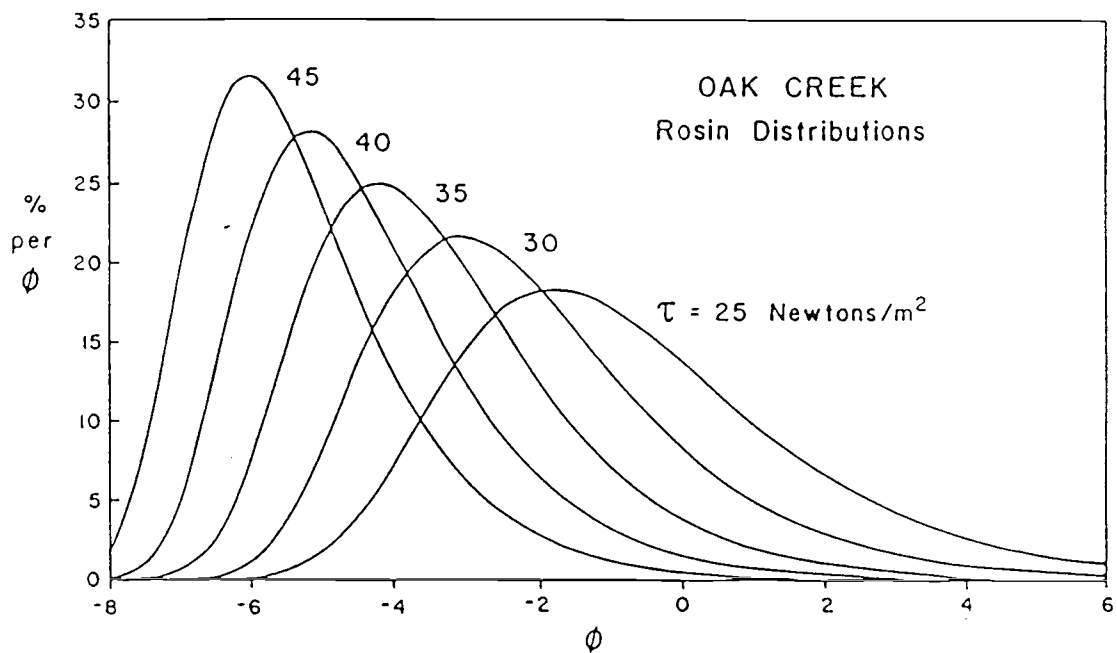


Figure 2-5. A series of frequency curves for ideal Rosin distributions for a range of flow stresses, τ , based on the k and s trends of Figures 2-3 and 2-4 so as to depict variations found in Oak Creek.

TOTAL TRANSPORT RATES OF GRAVELS IN OAK CREEK

The next step in the analysis is to determine how the total transport rate of gravel in Oak Creek depends on the flow hydraulics. There are many empirical bedload formulas and types of correlations that potentially could be used (Graf, 1971). However, the objective here is not to test formulations for the total transport, but to establish relationships which can be used to calculate transport rates of the different grain-size fractions. Therefore, simple correlations will be developed between the total gravel transport and the flow discharge or mean bed stress.

The total gravel transport rate per unit channel width, q_s , is plotted in Figures 2-6 and 2-7 as a function of the flow stress, respectively for the 22 samples collected at discharges in excess of 1 m³/sec and for the entire 66 samples obtained by Milhous (1973) during the winter 1971. The respective least-square correlations are:

$$q_s = 1.24 \times 10^{-19} \tau^{13.2} \quad [\text{discharge} > 1 \text{ m}^3/\text{sec}] \quad (7a)$$

and

$$q_s = 4.12 \times 10^{-14} \tau^{9.50} \quad [\text{all discharges}] \quad (7b)$$

Both correlations are very good, but there is seen to be some increase in data scatter at the lower flow-stress levels, Figure 2-7, those where the discharge is less than 1 m³/sec. Our subsequent calculations will utilize equation (7a) since we are interested here in transport at flow stages which exceed initiation of breakup of the bed pavement.

The analysis by Parker et al. (1982) of the 22 measurements sets for discharge > 1 m³/sec yielded an average empirical correlation for individual grain-size fractions which is comparable to equation (7a), but they found an exponent of 14.9. However, different size fractions individually yielded correlations which are equivalent to exponents ranging 7 to 17 (Diplas, 1987). Therefore, the results obtained here for the total gravel transport rates are consistent with those of Parker et al. and Diplas in their analysis of transport rates of sieve-size fractions.

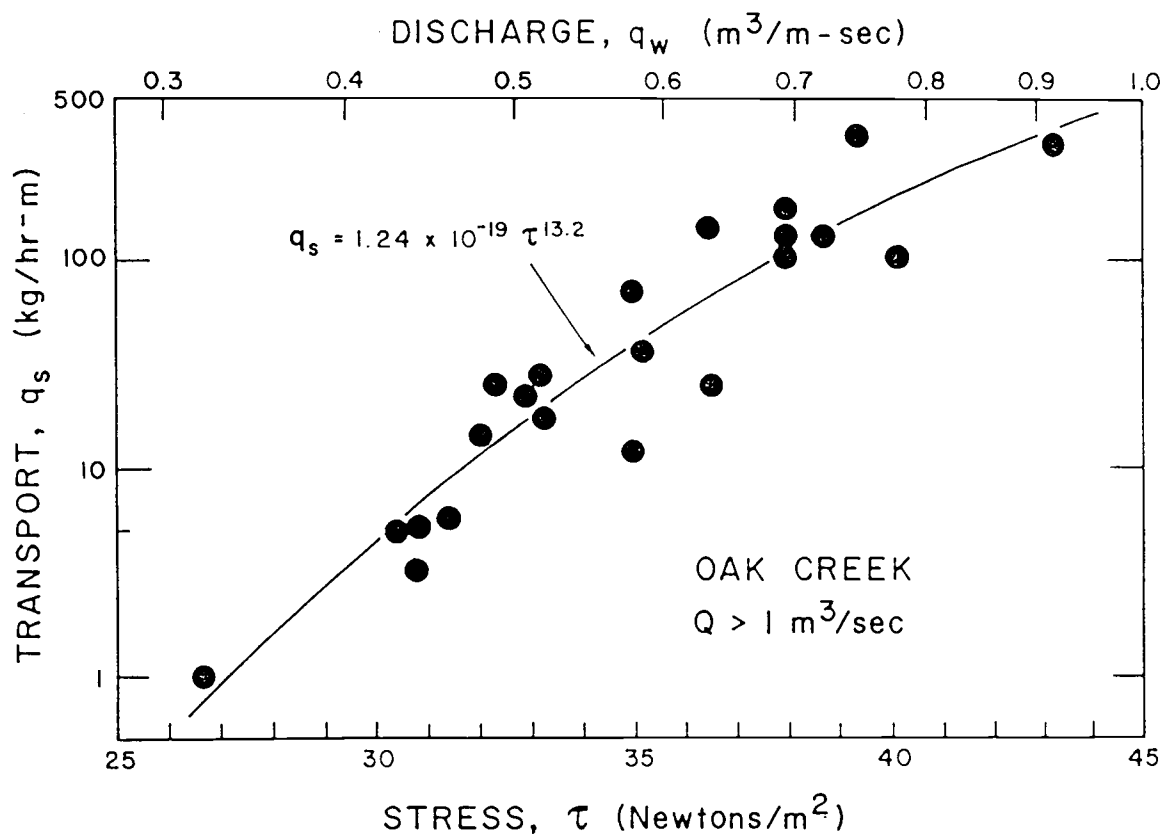


Figure 2-6. The mass transport rate of gravel per unit channel width in Oak Creek versus the flow stress. The measurements are the 22 subset of winter-1971 data obtained by Milhous (1973), those collected at discharges greater than $1 m^3/sec$ when the pavement is progressively breaking up.

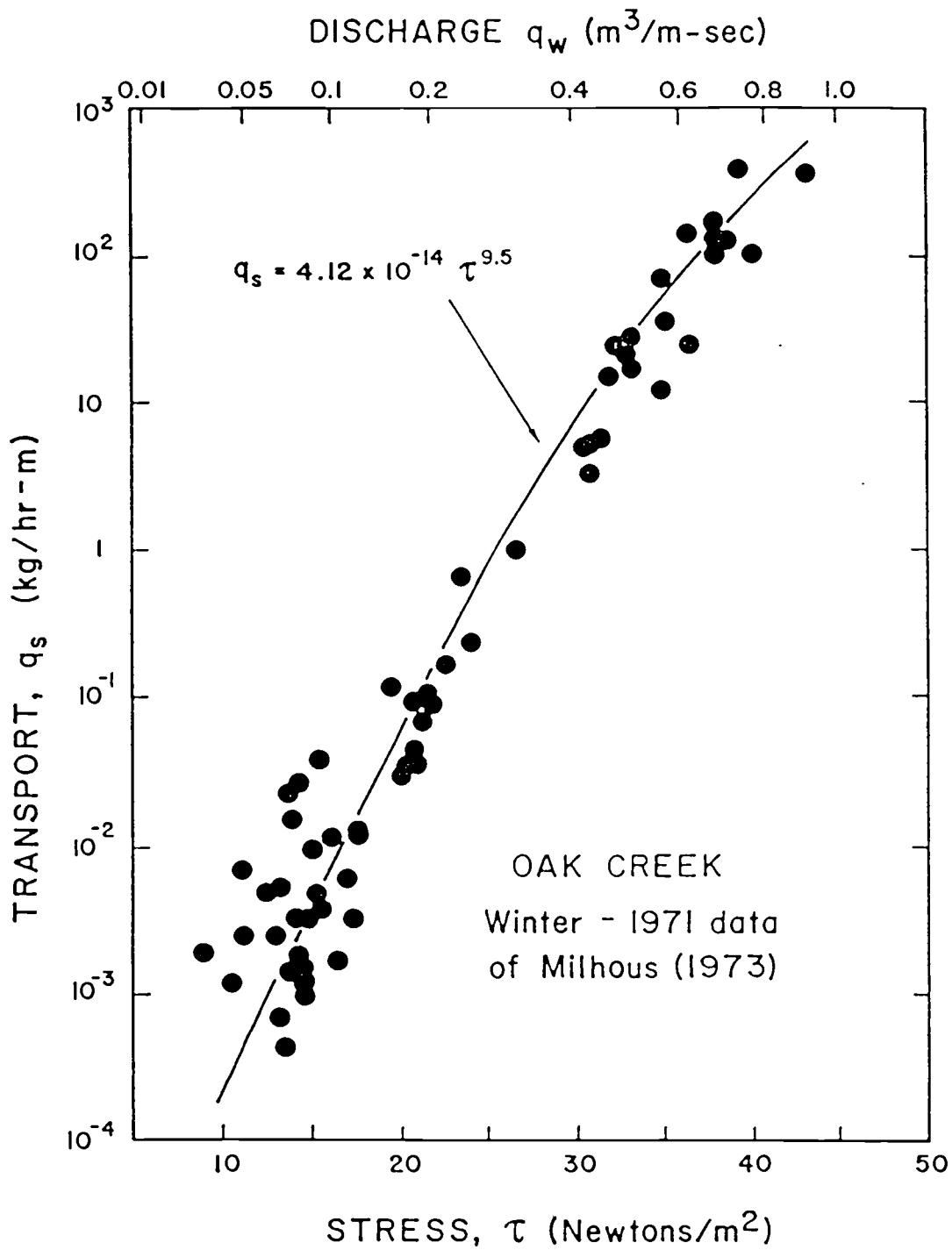


Figure 2-7. The mass transport rate of gravel per unit channel width in Oak Creek versus the flow stress. The measurements are the complete set of winter-1971 data obtained by Milhous (1973).

The discharge-based relationships equivalent to equations (7a) and (7b) are:

$$q_s = 989 q_w^{6.80} \quad [\text{discharge} > 1 \text{ m}^3/\text{sec}] \quad (8a)$$

and

$$q_s = 20.8 q_w^{4.36} \quad [\text{all discharges}] \quad (8b)$$

Equation (8a) is compared with the data in Figure 2-8 where agreement is again seen to be good. It has been established that 21 of the 66 measurements of discharge in the winter-1971 data of Milhous (1973) were apparently affected by a mis-calibration. The flow-stress measurements are correct, so that equation (3) has been used to infer q_w discharges for those 21 data sets (12 of which appear in Figure 2-8).

Scholkitsch has derived correlations between q_s to q_w for gravel transport (Graf, 1971), which have the form

$$q_s = C (q_w - q_c) \quad (9)$$

where q_c is a critical discharge for initiation of grain movement. Bathurst et al. (1983) have established this type of relationship for flume data, and have applied it with some degree of success to large rivers of steep slope. The best fit we have been able to achieve with the Oak Creek data is

$$q_s = 1355(q_w - q_c)^{3.41} \quad (10)$$

where $q_c = 0.22 \text{ m}^3/\text{m}\cdot\text{sec}$, which is the discharge per unit channel width that corresponds approximately to the critical $1 \text{ m}^3/\text{sec}$ total discharge necessary to initiate breakup of the bed pavement (and corresponds more closely to the 42 cfs critical value given by Milhous). Agreement with the data in Figure 2-8 is seen to be reasonable, but the 3.41 exponent in equation (10) is substantially greater than the exponent 1 inherent in the direct proportionality of Scholkitsch's equation (9). The reason for this is not known, but similar differences have been found for flow-competence relationships yielding discharges from transported grain sizes for the Oak Creek data (Komar, 1989).

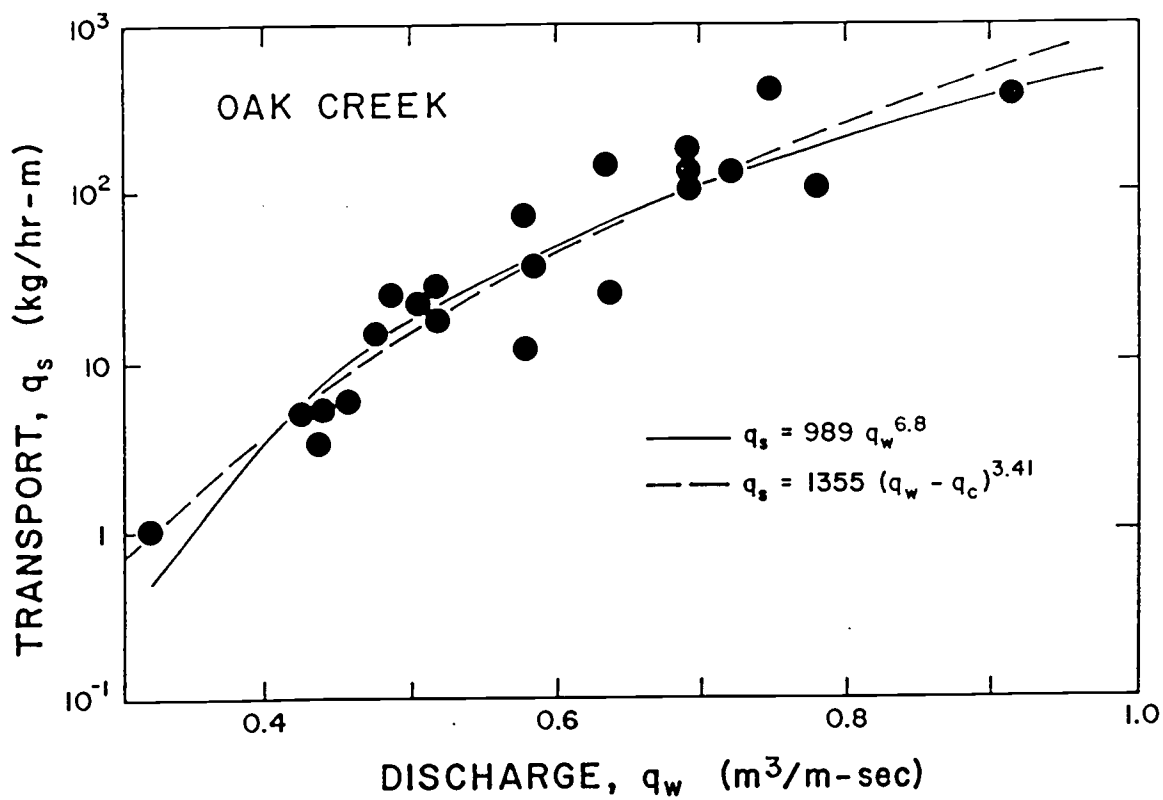


Figure 2-8. A Schoklitsch-type analysis of the Oak Creek gravel transport for the subset of winter-1971 data collected by Milhous (1973) when discharges exceeded $1 m^3/sec$.

TRANSPORT RATES OF GRAIN-SIZE FRACTIONS

It is a simple matter to combine the above results for the total gravel transport with the earlier findings concerning the changing grain-size distributions, to obtain a formulation for the distribution of transport rates of the different size fractions. One such solution is obtained by combining equation (7a) for the total transport, q_s , with equation (1), the cumulative form of the Rosin distribution, to yield

$$G_{sj}(D_i, \tau) = q_s(\tau) [100 \exp\{-[D_i/k(\tau)]^s(\tau)\}] \quad (11)$$

where functional dependencies on the flow stress τ and size fraction $x = D_i$ are indicated by the parentheses. The bedload transport rate within the size fraction larger than D_1 but smaller than D_2 at a specified stress τ is then calculated as $G_{s2}(D_2, \tau) - G_{s1}(D_1, \tau)$. The frequency curve of the bedload transport distribution can be obtained by differentiating $G_{sj}(D_i, \tau)$ of equation (11) with respect to D_i , or by combining $q_s(\tau)$ with the frequency grain-size distribution of equation (2a) to yield the fraction transport rate,

$$q_{sj}(D_i, \tau) = q_s(\tau) f_j(D_i, \tau) \quad (12a)$$

$$q_{sj}(D_i, \tau) = 100 q_s(\tau) [s(\tau)/k(\tau)] [D_i/k(\tau)]^{s(\tau)-1} \exp\{-[D_i/k(\tau)]^s(\tau)\} \quad (12b)$$

Frequency distributions are shown in Figure 2-9, calculated for five bed shear stresses ranging from 30 to 40 Newtons/m². Only a limited range of results can be presented on one graph, since the transport rises at an extreme rate as τ increases. The series of frequency curves reflect the variability of the transport rates for the different grain sizes together with the progressive shift and changing form of the resulting distributions of grain sizes. The total transport rate of gravel at a given stress value is equal to the total area under the curve.

The results of this analysis can be tested against the measured transport rates of size fractions determined by Milhous (1973), but this requires degrading the continuous frequency curves obtained here back into sieve intervals. This has been done

for the coarsest ten sieve fractions reported by Milhous, and the results are shown in Figure 2-10 as predicted versus measured rates. The correlation is very good, especially considering that the predictions rely only on the flow stress without extensive parameterization of other hydraulic factors.

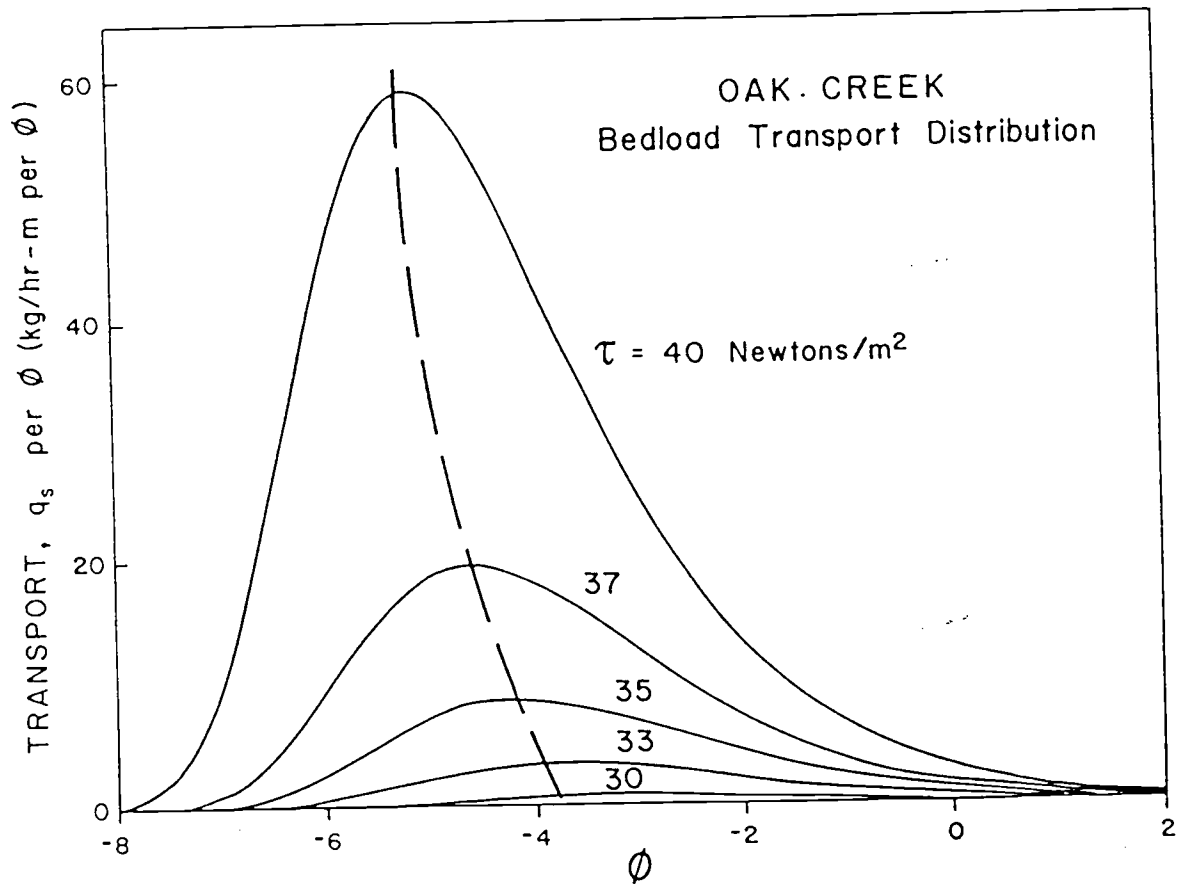


Figure 2-9. Frequency distributions of fractional transport rates of gravels in Oak Creek, calculated for a range of flow stresses, τ . The curves are Rosin distributions with the k and s parameters related to τ in Figure 2-4. The total transport rate is represented by the area under the curve, and was calculated from equation (7a). The dashed line follows the distribution peaks, and shows how it shifts to coarser sizes as the flow stress increases.

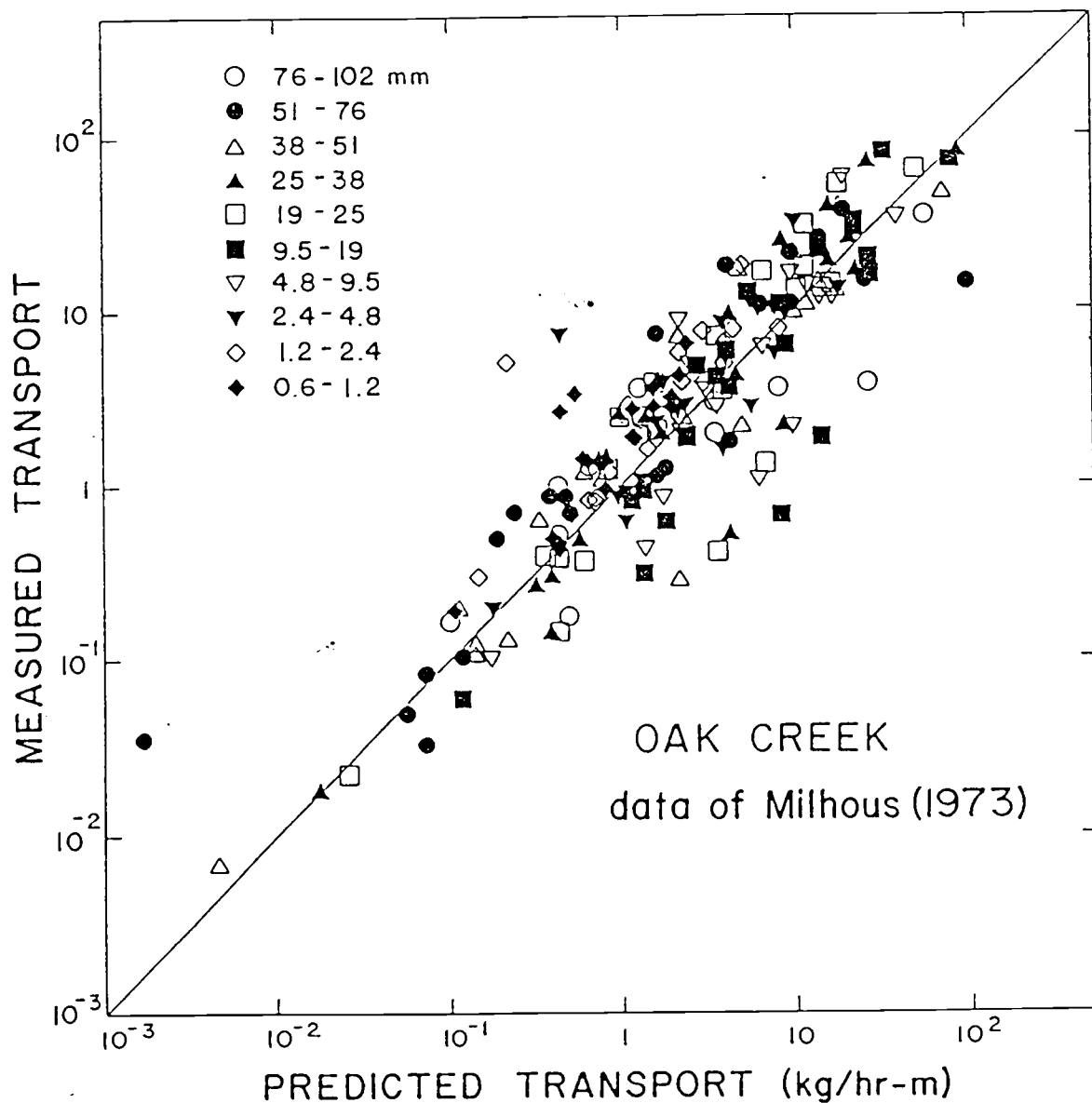


Figure 2-10. Measured transport rates of different sieve-size fractions as determined directly from the data of Milhous (1973) for the subset of winter-1971 data when discharges were greater than $1 \text{ m}^3/\text{sec}$, versus predicted rates calculated from the Rosin distributions of fractional transport rates analyzed in this study.

COMPARISON WITH PARKER ET AL. (1982) AND DIPLAS (1987)

Parker et al. (1982) and Diplas (1987) also based their gravel-transport relationships on the thesis data of Milhous (1973), and therefore a direct comparison with our analysis is in order. The equations developed by Parker et al. and Diplas were placed in nondimensional form, complicating direct comparisons. However, it can be shown that their dimensionless equations may be algebraically reduced to a proportionality

$$q_{si}(D_i, \tau) = q_s(\tau) f_{ir} \propto \tau^{m+3/2} f_{ir} \quad (13a)$$

which is similar to our equation (12) simplified to

$$q_{si}(D_i, \tau) = q_s(\tau) f_i(D_i, \tau) \propto \tau^{13.2} f_i(D_i, \tau) \quad (13b)$$

when the total transport q_s is given by equation (7a). In equation (13a), f_{ir} represents the frequencies of sieve fractions of a reference grain-size distribution, taken by Parker et al. and Diplas as the size distribution of the subpavement bed material (Figure 2-1). Therefore, the most important distinction between equations (13a) and (13b) is that f_{ir} in the former represent fixed quantities, whereas in our approach the $f_i(D_i, \tau)$ frequencies are for the bedload grain-size distributions which change depending on the flow stress τ or discharge. With the equal-mobility assumptions made by Parker et al., the exponent in equation (13a) is $m + 3/2 = 14.8$. It is apparent then that the equal-mobility analysis in effect accounts for the total transport being proportional to $\tau^{14.8}$, and that this transport is apportioned into the subpavement f_{ir} size distribution. The short-coming of this approach is that all bedload samples have grain-size distributions identical to the subpavement (f_{ir}), and do not change with varying flow discharge and bed stress. This problem with the equal-mobility assumption was recognized by Parker et al. in noting the observed variations in the mean diameters of the bedload grain-size distributions.

Diplas (1987) modified the Parker et al. (1982) analysis by accounting for variations in the m exponent of equation (13a) for the several sieve fractions by setting $m = 13.71(D_i / D_{50})^{0.3214}$ where the sieve size D_i is normalized to the median diameter D_{50} of the subpavement bed material. Diplas showed that this change in the analysis is successful in accounting for the observed variations in mean diameters of the Oak Creek bedload samples, and therefore does represent an improvement over the equal-mobility assumptions. However, making the exponent m of equation (13a) depend on D_i increases the contrast with our approach, equation (13b), where the exponent is fixed and observed changes in bedload grain-size distributions are instead accounted for by variations in $f_i(D_i, \tau)$. We feel that our approach is preferable in that equation (13b) more clearly separates out the total gravel transport rate which is proportional to $\tau^{13.2}$ (eq. 7a), and demonstrates how the grain-size distributions of bedload samples evolve with flow stage.

It can also be shown that equation (13b) from our analysis is algebraically equivalent to

$$W_i^* \propto \left(\frac{\tau}{\tau_r} \right)^{11.7} \frac{f_i(D_i, \tau)}{f_{i,r}} \quad (14)$$

where W_i^* is the dimensionless transport rate as defined by Parker et. al. Here we have the variable $f_i(D_i, \tau)$ distributions of the bedload compared with the fixed $f_{i,r}$ reference distribution of the bed material, and the measured flow stress τ is divided by a reference flow stress, τ_r . Important in the analysis of Parker et al. is the use of a low-level reference transport rate which has the grain-size distribution of the subpavement bed material. The problem is that this subpavement distribution is not found in the bedload samples, especially not at the low stages of their reference transport. In contrast, equation (14) from our analysis suggest that the reference τ_r flow stress be set at a high

flow stage, that at which bedload grain-size distributions effectively become the same as the bed material, some combination of the pavement and subpavement.

NORMALIZATION OF THE RESULTS

As developed above, the approach is suitable only to calculations of gravel-transport distributions in Oak Creek. Attention needs to be given to normalizing the results so as to broaden potential applications. Much attention has been given to developing standard relationships for the total transport rate and to testing their consistency from one stream to another (Graf, 1971). We can accept those results as generalizing half of equations (11) and (12), that involving the computations of $q_s(\tau)$. Therefore, normalization of the analysis to broaden its application must focus on the changing bedload grain-size distributions.

The dimensionless equation (14) offers one approach, that which corresponds most closely to the analysis of Parker et al. (1982) and Diplas (1987). Another approach involves normalizing the k and s parameters of the bedload Rosin distributions to the values for the bed material. Accordingly, equations (4a) and (6a) become

$$k/k_r = a(\tau/\tau_r)^b \quad (15a)$$

and

$$s/s_r = c(\tau/\tau_r)^d \quad (15b)$$

where the subscript r denotes a reference value related to the bed material, and a , b , c and d are empirical coefficients. Higher-order descriptions would involve modifying equation (5) to a regression of k/k_r versus τ/τ_r . As discussed above, we are interested in a high flow stage as the reference condition, a stress τ_r at which the grain-size distribution of the bedload achieves essentially the same distribution as the bed material (denoted by k_r and s_r). Oak Creek offers complications in the selection of the reference combination, k_r , s_r and τ_r , due to the separation of the bed material into a pavement and subpavement. It was seen in Figures 2-3 and 2-4 that the k and s values of the bedload distributions appear to be approaching levels that are intermediate between the respective values of the pavement and subpavement, an expected result in that bedload at

high flow stages will recombine those two bed-material distributions. The trends of the curves in Figures 2-3 and 2-4 suggest that at a high stress level ($\tau_r \approx 45 \text{ N/m}^2$), $k_r \approx 35 \text{ mm}$ and $s_r \approx 1.2$; it is unfortunate that the measurements of Milhous (1973) do not extend to somewhat higher flow stages so as to better establish how the trends of k and s level off. These particular k_r and s_r values are obtained by combining 30% pavement and 70% subpavement. When used in equations (15) together with the k and s of the bedload samples, we obtain $a = 1.78$, $b = 5.00$, $c = 1.02$ and $d = 0.91$ for the empirical coefficients.

Although best success has been achieved in Oak Creek with the Rosin distribution, alternate choices such as Gaussian distributions might show better agreement in other streams. In each stream the analysis will involve documenting how the bedload grain-size distributions relate to the bed-material source at different flow stages, just as undertaken here for Oak Creek.

It remains to be established whether this normalizing procedure to a reference bed-material distribution yields a degree of conformity between changing bedload grain-size distributions in different streams. We can anticipate that there will be differences from one stream to another, because the empirical coefficients in equations (15) reflect the patterns of grain sorting in the particular stream. Those sorting patterns will differ to some degree from one stream to another, especially from one that has a well-developed pavement compared with another that has no pavement. Therefore, changes in the coefficients from stream to stream should not be taken as necessarily indicating a failure of the normalizing procedure, but as a result that more accurately describes the nature of the sorting processes and changing bedload transport distributions.

SUMMARY AND DISCUSSION

A bedload transport function has been developed for individual size fractions of gravels in Oak Creek, Oregon. The general approach couples standard formulas for the total bedload transport rate with descriptions of changing bedload grain-size distributions. With this approach, the fractional transport rates can be calculated as smooth distributions rather than as histograms representing transport rates of individual sieve fractions. In focusing on how grain sizes reflect the flow discharge or mean bed stress, the approach joins techniques of flow-competence evaluations with formulations which yield total transport rates.

The present approach provides a distinct alternative to the analysis procedures of Parker et al. (1982) and Diplas (1987) which also employed the Oak Creek data of Milhous (1973). The Parker et al. equal mobility analysis does not account for changing bedload grain sizes, and accordingly was recognized by them as only a first-order solution. Diplas developed a higher-order analysis which does account for changes in the mean grain sizes of the bedload samples with flow stage, but the modification involves a dependence on a representative sieve-size diameter of the exponents in the empirical correlations. That empirical modification obscures the actual processes involved in the selective entrainment and transport, those which give rise to the differential transport rates and changing grain-size distributions. The approach developed here relates more directly to the physical processes of grain entrainment and transport as reflected in the bedload grain sizes.

A series of bedload-transport rating curves can be constructed for fluvial environments to facilitate the evaluation of fractional transport rates at different flow conditions. The curves may vary as the hydraulic and geological factors change for different streams. Comparisons of the curves for different reaches within the same river should lead to a better understanding of how the differential bedload transport

varies along its length, and to what extent selective transport is responsible for observed downstream decreases in bed-material grain sizes.

REFERENCES

- Bagnold, R.A. (1937) The size-grading of sand by wind: *Proc. Royal Soc. London*, series A, 163, 250-264.
- Baker, V.R. & Ritter, D.F. (1975) Competence of rivers to transport coarse bedload material: *Bull. Geol. Soc. Amer.*, 86, 975-978.
- Barndorff-Nielsen, O. (1977) Exponential decreasing distributions for the logarithm of particle size: *Proc. Royal Soc. London*, series A, 353, 401-419.
- Bathurst, J.C., Graf, W.H. & Cao, H.H. (1983) Bedload discharge equations for steep mountain rivers: In *Sediment Transport in Gravel-Bed Rivers*, C.R. Thorne et al. (editors), John Wiley & Sons,
- Bennett, J.G. (1936) Broken coal: *Jour. Inst. Fuel*, 10, 22-39.
- Beschta, R.L. (1983) Sediment and organic matter transport in mountain streams of the Pacific Northwest: In *Proc. of the D.B. Simons Symposium on Erosion and Sedimentation*, Simons, Li & Assoc., Ft. Collins, Co., 169-189.
- Christiansen, C., Blaesild, P., and Dalsgaard, K. (1984) Re-interpreting 'segmented' grain-size curves: *Geol. Mag.*, 121, 47-51.
- Costa, J.E. (1983) Paleohydraulic reconstruction of flash-flood peaks from boulder deposits in the Colorado Front Range: *Bull. Geol. Soc. Amer.*, 94, 986-1004.
- Dapples, E.C. (1975) Laws of distribution applied to sand sizes: *Geol. Soc. Amer. Memopir* 142, 37-61.
- Davis, J.C. (1986) *Statistics and Data Analysis in Geology*: John Wiley & Sons, New York.
- Diplas, P. (1987) Bedload transport in gravel-bed streams: *Jour. Hydraulic Eng., Amer. Soc. Civil Engr.*, 113, 277-292.
- Einstein, H.A. (1950) The bedload function for sediment transportation in open channels: Tech. Bull. 1026, U.S. Dept. of Agriculture.

- Geer, M. R. & Yancy, H.F. (1938) Expression and interpolation of size composition of coal: *Amer. Inst. Min. and Met. Eng.*, Tech. Publ. 948.
- Geer, M. R. & Yancy, H.F. (1938) Expression and interpolation of size composition of coal: *Amer. Inst. Min. and Met. Eng.*, Tech. Publ. 948.
- Graf, W.H. (1971) *Hydraulics of Sediment Transport*: McGraw-Hill Book Co., New York, 513 p.
- Grass, A.J. (1971) Structural features of turbulent flow over smooth and rough boundaries: *J. Fluid Mech.*, **50**, 233-255.
- Ibbeken, H. (1983) Jointed source rocks and fluvial gravels controlled by Rosin's law: A grain size study in Calabria, South Italy: *J. Sedim. Petrol.*, **53**, 1213-1231.
- Jackson, R.G. (1975) Mechanisms and hydrodynamic factors of sediment transport in alluvial streams: In *Research in Fluvial Geomorphology*, R. Davidson-Arnott & W. Nickling (eds.), Geo Abstracts Ltd., Norwich, 9-44.
- Kittleman, L.R. (1964) Application of Rosin's distribution in size frequency analysis of clastic rocks: *J. Sedim. Petrol.*, **34**, 483-502.
- Klovan, J.E. (1966) The use of factor analysis in determining depositional environments from grain-size distributions: *J. Sedim. Petrol.*, **36**, 115-125.
- Komar, P.D. (1986) 'Breaks' in grain-size distributions and applications of the suspension criterion to turbidites: *Sedimentology*, **33**, 438-440.
- Komar, P.D. (1987) Selective gravel entrainment and the empirical evaluation of flow competence: *Sedimentology*, **34**, 1165-1176.
- Komar, P.D. (1989) Flow-competence evaluations of the hydraulic parameters of floods: An assessment of the technique: in *Floods - Hydrological, Sedimentological and Geomorphological Implications*, eds. K. Beven and P. Carling, John Wiley & Sons, Ltd.
- Krumbein, W.C. & Tisdell, F.W. (1940) Size distribution of source rocks of sediments: *Amer. Jour. Sci.*, **238**, 296-305.

- Leinen, M., and Piasias, N. (1984) An objective technique for determining end-member composition and for partitioning sediments according to their sources: *Geochem., Cosmochem. Acta*, **40**, 671-676.
- Leroy, S.D. (1981) Grain-size and moment measures: A new look at Karl Pearson's ideas on distributions: *J. Sedim. Petrol.*, **51**, 625-630.
- Milhous, R. T. (1973) *Sediment transport in a gravel-bottomed stream*: Ph.D. thesis, Oregon State University, Corvallis, 232 pp.
- Parker, G., Klingeman, P.C. & McLean, D.G. (1982) Bedload and size distribution in paved gravel-bed streams: *Jour. Hydraulics Div., Amer. Soc. Civil Engrs.*, **108**, HY4, 544-571.
- Poreh, M., Sagiv, A. & Seginer, I. (1970) Sediment sampling efficiency of slots: *J. Hydrs. Div., Amer. Soc. Civil Engrs.*, **96**, HY10, 2065-2078.
- Proffitt, G.T., & Sutherland, A.J. (1983) Transport of non-uniform sediment: *Jour. of Hydraulic Research*, **21**, 33-43.
- Robinson, A.R. (1962) Vortex tube sand trap: *Trans. Amer. Soc. Civil Engrs.*, **127**, 391-425.
- Rosin, P. & Rammler, E. (1933) Laws governing the fineness of powered coal: *J. Inst. Fuel.*, **7**, 29-36.
- Schleyer, R. (1987) The goodness-of-fit to ideal Gauss and Rosin distributions: A new grain-size parameter: *J. Sedim. Petrol.*, **57**, 871-880.
- Visher, G.S. (1969) Grain size distributions and depositional processes: *J. Sedim. Petrol.*, **39**, 1074-1106.
- Wolcott, J. (1988) Nonfluvial control of bimodal grain-size distributions in river-bed gravels: *J. Sedim. Petrol.*, **58**, 979-984.

APPENDICES

APPENDIX A:

GRAIN-SIZE AND HYDRAULIC PARAMETERS

Table A-1: Grain-size parameters and hydraulic data for the bedload samples reanalyzed in this thesis. Winter-1971 data of Milhous(1973).

Sample Number	Discharge (m ³ /sec)	Bed shear stress (newton/m ²)	k (mm)	s	Goodness-of-fit	
					Rosin	Gaussin
armor			65.54	1.47	97.89	96.38
subarmor			29.10	0.82	96.78	95.21
1	0.153	8.92	*			
2	0.238	11.04	1.21	1.10	95.12	97.90
3	0.337	12.33	1.68	1.06	94.85	97.73
4	0.391	13.64	1.99	0.95	95.40	98.35
5	0.447	15.33				
6	0.382	13.87	2.04	1.09	96.00	98.53
7	0.323	12.59	1.21	1.18	95.56	98.32
8	0.275	11.17				
9	0.227	10.54	1.46	1.07	95.29	97.92
10	2.605	37.96	31.78	1.47	98.80	97.61
11	2.605	37.96	22.90	1.12	99.49	98.04
12	2.633	37.96				
13	2.832	40.10	32.12	1.08	97.78	95.76
14	3.398	43.18	31.40	1.45	98.90	97.77
15	1.897	33.16	17.00	0.94	98.60	96.47
16	1.812	32.26	12.61	0.93	98.65	98.32
17	0.906	23.42	6.47	0.86	97.30	98.67
18	0.736	21.44	3.55	1.06	96.16	98.57
19	0.765	21.73	3.96	0.95	97.01	98.76
20	0.680	20.86	3.31	1.04	95.85	98.39
21	0.708	21.15	3.55	1.06	95.92	98.21
22	0.680	20.66	3.56	1.06	96.29	98.93
23	1.756	31.96				
24	1.699	31.36				
25	1.529	30.77	6.12	0.90	96.19	98.17
26	1.161	26.62	3.44	1.10	96.24	97.69
27	0.821	22.54	2.10	1.45	97.69	98.75
28	0.623	20.28	1.74	1.50	98.14	98.52
29	0.453	17.49	1.53	1.39	98.30	99.22
30	0.368	16.92	1.22	1.49	98.16	99.29
31	0.331	16.06	1.05	1.70	98.31	99.41
32	0.283	15.04	1.55	1.18	97.03	98.83
33	0.232	14.19	1.30	1.34	97.33	99.44
34	0.241	14.19	1.15	1.29	97.64	99.38
35	0.651	20.57	1.13	1.50	97.60	99.11
36	0.453	17.49	1.24	1.50	97.64	99.12
37	0.312	15.49				
38	0.252	14.63	1.93	1.04	95.98	98.52
39	0.221	14.32				
40	0.252	14.47				
41	0.193	12.92	2.15	1.19	97.49	99.36
42	0.198	13.20	3.57	0.98	96.56	99.04
43	0.218	13.48				
44	0.235	13.76				
45	0.204	13.20	1.88	1.28	96.48	98.59
46	0.238	14.04				
47	0.300	15.20	2.82	0.99	96.83	99.34
48	0.269	14.76				

Table A-1 continued

Sample Number	Discharge (m ³ /sec)	Bed shear stress (newton/m ²)	k (mm)	s	Goodness-of-fit	
					Rosin	Gaussin
49	0.232	14.04	4.14	0.84	97.73	99.31
50	0.263	14.47	1.60	1.08	97.73	99.31
51	0.566	19.41				
52	0.600	19.99	1.50	1.37	96.99	98.44
53	0.419	17.21				
54	0.362	16.35				
55	0.538	24.07				
56	1.756	34.95				
57	2.039	36.51				
58	2.605	38.69	32.12	0.95	97.35	95.22
59	2.209	39.36	31.78	1.21	99.19	97.49
60	1.529	35.13	16.39	0.97	98.19	98.06
61	1.331	33.24	16.37	0.94	98.95	97.30
62	1.020	30.77	9.38	0.84	98.35	98.80
63	1.076	30.47	9.00	0.86	97.73	98.68
64	1.444	32.86	15.03	0.91	98.66	97.46
65	1.756	34.95	24.25	0.95	98.14	97.36
66	2.096	36.44	29.22	1.01	98.39	96.27

* Grain-size parameters are not available for bimodal samples.

APPENDIX B:**ROSIN PAPER**

Appendix B

